

Demonstrating the Use of Small Uncrewed Aircraft Systems (Drones) Capabilities and Data for Iowa Transportation and Infrastructure Work

Pilot Project No. 3 – Use of Small Uncrewed Aircraft Systems for Erosion and Sediment Control Device Monitoring

Task Report | May 2026



IOWA STATE UNIVERSITY
Institute for Transportation

Sponsored by
Iowa Department of Transportation
and Federal Highway Administration
(SPR-RE24(010)-8H-00,
InTrans Project 24-904)

About the Program for Sustainable Pavement Engineering and Research

The overall goal of the Program for Sustainable Pavement Engineering and Research (PROSPER) is to advance research, education, and technology transfer in the area of sustainable highway and airport pavement infrastructure systems.

About the Institute for Transportation

The mission of the Institute for Transportation (InTrans) at Iowa State University is to save lives and improve economic vitality through discovery, research innovation, outreach, and the implementation of bold ideas.

Iowa State University Nondiscrimination Statement

Iowa State University does not discriminate on the basis of race, color, age, ethnicity, religion, national origin, pregnancy, sexual orientation, genetic information, sex, marital status, disability, or status as a U.S. Veteran. Inquiries regarding nondiscrimination policies may be directed to Office of Equal Opportunity, 2680 Beardshear Hall, 515 Morrill Road, Ames, Iowa 50011, telephone: 515-294-7612, email: eooffice@iastate.edu.

Disclaimer Notice

The contents of this report reflect the views of the authors, who are responsible for the facts and the accuracy of the information presented herein. The opinions, findings and conclusions expressed in this publication are those of the authors and not necessarily those of the sponsors.

The sponsors assume no liability for the contents or use of the information contained in this document. This report does not constitute a standard, specification, or regulation.

The sponsors do not endorse products or manufacturers. Trademarks or manufacturers' names appear in this report only because they are considered essential to the objective of the document.

Quality Assurance Statement

The Federal Highway Administration (FHWA) provides high-quality information to serve Government, industry, and the public in a manner that promotes public understanding. Standards and policies are used to ensure and maximize the quality, objectivity, utility, and integrity of its information. The FHWA periodically reviews quality issues and adjusts its programs and processes to ensure continuous quality improvement.

Iowa DOT Statements

The Iowa Department of Transportation (DOT) ensures non-discrimination in all programs and activities in accordance with Title VI of the Civil Rights Act of 1964. Any person who believes that they are being denied participation in a project, being denied benefits of a program, or otherwise being discriminated against because of race, color, national origin, gender, age, or disability, low income and limited English proficiency, or if needs more information or special assistance for persons with disabilities or limited English proficiency, please contact Iowa DOT Civil Rights at 515-239-7970 or by email at civil.rights@iowadot.us.

The preparation of this report was financed in part through funds provided by the Iowa DOT through its "Second Revised Agreement for Management of Research Conducted by Iowa State University for the Iowa Department of Transportation" and its amendments.

The opinions, findings, and conclusions expressed in this publication are those of the authors and not necessarily those of the Iowa DOT or the U.S. DOT FHWA.

Technical Report Documentation Page

1. Report No. InTrans Project 24-904	2. Government Accession No.	3. Recipient's Catalog No.	
4. Title and Subtitle Demonstrating the Use of Small Uncrewed Aircraft Systems (Drones) Capabilities and Data for Iowa Transportation and Infrastructure Work: Pilot Project No. 3 – Use of Small Uncrewed Aircraft Systems for Erosion and Sediment Control Device Monitoring		5. Report Date May 2026	
		6. Performing Organization Code	
7. Author(s) Kunle S. Oguntoye (orcid.org/0009-0002-9993-3304), Md Abdullah All Sourav (orcid.org/0000-0003-3387-740X), Rajrup Mitra (orcid.org/0000-0003-1937-7222), Abby Jenkins (orcid.org/0009-0007-5860-421X), Halil Ceylan (orcid.org/0000-0003-1133-0366), Sunghwan Kim (orcid.org/0000-0002-1239-2350), Berk Gulmezoglu (orcid.org/0000-0001-6268-6325), Yunjeong (Leah) Mo (orcid.org/0000-0002-5162-2235) and Colin N. Brooks (orcid.org/0000-0003-4544-2569)		8. Performing Organization Report No. InTrans Project 24-904	
9. Performing Organization Name and Address Program for Sustainable Pavement Engineering and Research (PROSPER) Institute for Transportation Iowa State University 2711 South Loop Drive, Suite 4700 Ames, IA 50010-8664		10. Work Unit No. (TRAIS)	
		11. Contract or Grant No.	
12. Sponsoring Organization Name and Address Iowa Department of Transportation Federal Highway Administration 800 Lincoln Way 1200 New Jersey Avenue, SE Ames, IA 50010 Washington, DC 20590		13. Type of Report and Period Covered Task Report	
		14. Sponsoring Agency Code SPR-RE24(010)-8H-00	
15. Supplementary Notes Visit https://prosper.intrans.iastate.edu/ for color pdfs of this and other research reports.			
16. Abstract Erosion and sediment control devices (ESCDs) are commonly installed on construction projects to mitigate the effects of runoff and sediment transport in downstream environments. Regulatory agencies such as the U.S. Environmental Protection Agency require these devices to be frequently inspected and maintained promptly when deficiencies are observed or when extreme upcoming precipitation events are expected. Smaller construction sites (less than 0.1 hectares) typically have fewer ESCDs, enabling effective routine field inspections. However, performing similar field inspections on larger construction sites is considerably more challenging due to their spatial distribution and the variety of ESCDs deployed across these sites. Other challenges include difficulty in physically locating these ESCDs due to complex or unstable terrain, potential exposure of inspection personnel to hazardous substances, and the significant amount of time required to navigate large sites and conduct detailed inspections. To address these limitations, this study investigated the use of small uncrewed aerial systems (sUAS) as a remote sensing platform for ESCD inspection and monitoring. The objective of this study was to develop a rapid data collection and processing pipeline that enables inspection personnel to efficiently evaluate site conditions and ESCD performance, supporting timely, informed decision-making. We deployed multiple sUAS platforms capable of producing high-resolution orthophotos for remote visual inspection and multispectral data for further analysis. These analyses included estimating vegetation growth on sloped terrain and quantifying the sediment accumulated near barriers such as silt fences and check dams. Digital elevation models (DEM) derived from the processed sUAS data also offered valuable insights into surface topography and flow patterns, enabling assessment of upstream and downstream conditions and improving understanding of how effectively ESCDs are functioning through quantitative analysis.			
17. Key Words drones—erosion and sediment control devices—infrastructure assessment— multispectral imagery		18. Distribution Statement No restrictions.	
19. Security Classification (of this report) Unclassified.	20. Security Classification (of this page) Unclassified.	21. No. of Pages 49	22. Price NA

DEMONSTRATING THE USE OF SMALL UNCREWED AIRCRAFT SYSTEMS (DRONES) CAPABILITIES AND DATA FOR IOWA TRANSPORTATION AND INFRASTRUCTURE WORK

PILOT PROJECT NO. 3 - USE OF SMALL UNCREWED AIRCRAFT SYSTEMS FOR EROSION AND SEDIMENT CONTROL DEVICE MONITORING

**Pilot Project Report
May 2026**

Principal Investigator

Halil Ceylan, Professor and Director
Program for Sustainable Pavement Engineering and Research (PROSPER),
Institute for Transportation, Iowa State University

Co-Principal Investigators

Sunghwan Kim, Research Scientist, Institute for Transportation, Iowa State University
Berk Gulmezoglu, Assistant Professor, Electrical and Computer Engineering, Iowa State University
Yunjeong (Leah) Mo, Assistant Professor, Civil, Construction and Environmental Engineering, Iowa State University
Colin N. Brooks, Transportation Practice Area Leader, Michigan Tech Research Institute (MTRI),
Michigan Technological University

Research Associates

Md Abdullah All Sourav, Kunle Oguntoye, Rajrup Mitra, Abby Jenkins, Richard Dobson, Samuel Berger

Authors

Kunle S. Oguntoye, Md Abdullah All Sourav, Rajrup Mitra, Abby Jenkins, Halil Ceylan, Sunghwan Kim,
Berk Gulmezoglu, Yunjeong (Leah) Mo, and Colin N. Brooks

Sponsored by
Iowa Department of Transportation and Federal Highway Administration
(SPR-RE24(010)-8H-00)

Preparation of this report was financed in part
through funds provided by the Iowa Department of Transportation
through its Research Management Agreement with the Institute for Transportation
(InTrans Project 24-904)

A report from
Program for Sustainable Pavement Engineering and Research (PROSPER)

Iowa State University
2711 South Loop Drive, Suite 4700
Ames, IA 50010-8664
Phone: 515-294-8103 / Fax: 515-294-0467
<https://propser.intrans.iastate.edu>

TABLE OF CONTENTS

ACKNOWLEDGMENTS	ix
EXECUTIVE SUMMARY	xi
INTRODUCTION	1
Background and Problem Statement.....	1
Goals and Objectives	2
STUDY AREA	3
DATA COLLECTION, PROCESSING, AND VISUALIZATION	7
sUAS Data Collection.....	7
sUAS Data Processing	9
sUAS Data Visualization	10
DEVICE MONITORING	12
Vegetation	12
Rock Check Dams.....	15
Silt Fences	20
Wattles	26
Stormwater Basins	28
SUMMARY AND LIMITATIONS	30
FUTURE RESEARCH DIRECTIONS	32
REFERENCES	34

LIST OF FIGURES

Figure 1. Iowa DOT representative with the ISU and MTRI research team	3
Figure 2. Grading project site in Mediapolis, Iowa	4
Figure 3. Grading project site in Oskaloosa, Iowa.....	5
Figure 4. Erosion and sediment control devices at Mediapolis Site 1, including silt fences and a check dam	5
Figure 5. Erosion and sediment control devices at Mediapolis Site 2, including wattles, a reseeded slope, and a check dam.....	6
Figure 6. Erosion and sediment control devices at the Oskaloosa site, including wattles	6
Figure 7. Data pipeline from collection to visualization.....	7
Figure 8. Web-based data viewing platform (Iowa State University version)	10
Figure 9. Web-based data viewing platform (MTRI version)	11
Figure 10. ArcGIS Pro proof-of-concept toolbox for automatic vegetation index estimations	13
Figure 11. Mediapolis Site 1 MSAVI results for demarcated area 1	14
Figure 12. Mediapolis Site 1 MSAVI results for demarcated area 2	14
Figure 13. Mediapolis Site 1 MSAVI results for demarcated area 3	15
Figure 14. Mediapolis Site 1 MSAVI results for demarcated area 4.....	15
Figure 15. Screenshot of ArcGIS Pro proof-of-concept toolbox for raster clipping and elevation analysis of a rock check dam.....	17
Figure 16. Flowchart showing line development for elevation sampling.....	17
Figure 17. Front elevation of a check dam, upstream and downstream	18
Figure 18. Side elevation of a check dam, upstream and downstream	18
Figure 19. Front and side elevations of a check dam at Mediapolis Site 1, upstream and downstream	19
Figure 20. Front and side elevations of a check dam at the Oskaloosa site, upstream and downstream	19
Figure 21. Automatic segmentation of rock check dam images using K-means clustering	20
Figure 22. Screenshot of ArcGIS Pro proof-of-concept toolbox for profile plotting of silt fence areas.....	21
Figure 23. Plotted profile of a silt fence with accumulated sediment in the upstream section.....	22
Figure 24. Plotted profile of a silt fence with no visible sediment in the upstream section	23
Figure 25. Plotted profile of a damaged silt fence	23
Figure 26. Vegetation index analysis of sediment accumulated near a silt fence.....	24
Figure 27. Overview of the global scenes from Mediapolis Site 1 and the Oskaloosa site.....	25
Figure 28. Close-up view of a silt fence at Mediapolis Site 1 from the global scene view	26
Figure 29. Wattle profile plot generated using ArcGIS Pro proof-of-concept toolbox	27
Figure 30. 3D view showing a close-up examination of a wattle.....	27
Figure 31. 2D orthophotos showing stormwater basins from Mediapolis Site 1.....	28
Figure 32. Measurement of the area of a stormwater basin	29

LIST OF TABLES

Table 1. Summary of visited sites and deployed sUAS platforms	8
---	---

ACKNOWLEDGMENTS

The authors gratefully acknowledge the Iowa Department of Transportation (Iowa DOT) for sponsoring this research and the Federal Highway Administration (FHWA) for the state planning and research (SPR) funds used for this project.

The project technical advisory committee members, Ed Bartels, Brandon Billings, Lee Bjerke, Curtis Carter, Khyle Clute, Chris Cromwell, Alex Davis, Michelle Fields, Vanessa Goetz, Brian Keierleber (former Buchanan County Engineer), Todd Kinney, Ronald Knoche, Tim McClung, Matthew Miller, Wes Musgrove, Tammy Nicholson, Scott Nixon, Greg Parker, Jesse Peterson, Melissa Serio, Derek Snead, Wade Weiss, Cedric Wilkinson, Bob Younie, and Andrew Zimmerman, are gratefully acknowledged for their guidance, support, and direction throughout the study.

The authors acknowledge with deep appreciation the Iowa DOT's unwavering support, and this appreciation is extended to all the enthusiastic and hardworking Iowa DOT engineers and technicians who carefully carried out all field data collection. The authors would also like to express their sincere gratitude to the members of the Michigan Tech Research Institute (MTRI) research team that participated in this project and other research team members from the Program for Sustainable Pavement Engineering and Research (PROSPER) at the Institute for Transportation (InTrans) at Iowa State University (ISU) for their assistance.

EXECUTIVE SUMMARY

The increasing use of small uncrewed aircraft systems (sUAS), also known as drones, in transportation infrastructure monitoring has validated the critical importance of this technology in modern engineering practice. sUAS technology offers significant benefits, including cost efficiency, enhanced safety, and improved productivity. While these advantages align with the goals of the Iowa Department of Transportation (Iowa DOT), the integration of sUAS into routine engineering practices carried out by the Iowa DOT is yet to be fully explored.

During a Technical Advisory Committee (TAC) meeting held on April 8, 2025, the TAC expressed its interest in exploring the benefits of sUAS technology for monitoring erosion and sediment control devices (ESCDs). Based on this interest, the research team conducted this third pilot project, whose primary aim was to evaluate the effectiveness of sUAS in the remote assessment of ESCDs, which can enable informed, rapid intervention to ensure compliance with U.S. Environmental Protection Agency guidelines and Iowa DOT requirements.

We collected high-quality aerial images using three different sUAS platforms: (1) a FreeFly Astro equipped with a Sony ILX-LR1 61 MP red/green/blue (RGB, or natural color) camera, (2) a DJI Mavic 3 Multispectral (M3M) equipped with a 20 MP RGB camera and built-in 5 MP 1/2.8-inch complementary metal-oxide semiconductor (CMOS) cameras having green, red, red edge, and near-infrared (NIR) narrow spectral bands, and (3) a DJI Mavic 2 Enterprise Advanced (M2EA) equipped with a built-in 48 MP quad-Bayer camera and a 640 X 512 stereo thermal sensor. Based on TAC recommendations, we collected sUAS data from two major construction grading projects in Iowa:

1. Two grading project sites located in Mediapolis, Iowa: Site 1 (41.037680, -91.169391) and Site 2 (41.012754, -91.174138)
2. A grading project site located in Oskaloosa, Iowa (41.315838, -92.699494)

We conducted preliminary inspections of the sites before full drone deployment. During these preliminary inspections, we assessed the sites' conditions, noting traffic volume, overhead power cables, undulating terrain, and the types and locations of installed ESCDs. This information helped us determine the altitudes of drone flights and the regions of interest at the sites.

The TAC briefed us that traditional field inspection of these ESCDs is typically conducted weekly to evaluate them for compliance with erosion control needs. Given that sUAS-collected images are a snapshot of the condition of a site at a given time, we aimed to develop a seamless and rapid prototype data processing pipeline that proceeds from data collection through data visualization, enabling inspection personnel to adequately inspect the ESCDs in a timely manner using a method similar to that used for field inspections. Further, prototype analysis frameworks were developed to evaluate the feasibility of monitoring ESCDs using processed sUAS data.

The recommendations, key findings, and lessons learned from this overall study are as follows:

- There are critical factors that must be adequately considered for a seamless and rapid transition from data collection to visualization. These factors broadly include the optimization of ground control points (GCP), sensor requirements, the need for weather monitoring, authorization requirements, and approval from related authorities
- High-resolution RGB imagery, multispectral imagery, and digital elevation models (DEMs) derived from the sUAS imagery using close-range photogrammetry are essential data for remote assessment of ESCDs.
- Normalized Difference Vegetation Index (NDVI) and Modified Soil Adjusted Vegetation Index (MSAVI) values derived from multispectral data proved to be effective in assessing vegetation coverage. These indexes could be easily adopted by the Iowa DOT for large-scale vegetation quantification with high accuracy.
- The use of DEM data showed promising performance in condition monitoring for rock check dams, silt fences, and wattle. However, the data tested for this evaluation were limited, and further work with data collected from different surfaces and under different weather and environmental conditions is warranted.
- 3D views of the sUAS imagery-derived RGB orthophotos could provide additional insight into the overall condition of ESCDs.

This work demonstrated the effectiveness of sUAS technology for monitoring ESCDs on a small scale. Of the 16 ESCDs listed by the Iowa DOT as commonly adopted devices on construction sites, only 5 had been installed at the sites we visited. Therefore, we conclude that additional data from additional sites need to be collected.

INTRODUCTION

Background and Problem Statement

The extensive use of small uncrewed aircraft systems (sUAS), commonly known as drones, in the transportation industry for remote sensing and infrastructure monitoring has validated the critical importance of this technology in modern engineering practice (Watts et al. 2012). This technology has been adopted by both government agencies and private entities responsible for highways, bridges, transportation infrastructure, and airports (Banić et al. 2019, Brooks et al. 2022, Fischer et al. 2020, Flammini et al. 2016, Mitra et al. 2025, Nooralishahi et al. 2021, Oguntoye et al. 2025, Pietersen et al. 2022, Sourav et al. 2024, Tan and Li 2019). For example, a wide variety of studies have been conducted on airfield pavement damage detection and rating and on the long-term use of sUAS to complement traditional infrastructure inspection processes (Oguntoye et al. 2023, 2025; Pietersen et al. 2022; Sourav et al. 2022, 2023a, 2023b, 2023c, 2024; Vidyadharan et al. 2017). These studies have also provided guidelines for adoption and have explored future potential applications (Sourav et al. 2024).

An application for which remote assessment technology may be well suited is the inspection of erosion and sediment control devices (ESCDs). Current monitoring practices rely on traditional inspection methods, in which inspectors conduct close-up field inspections and thoroughly profile each visited device. While this approach is adequate for smaller construction sites with a few spatially close devices, it becomes a bottleneck when larger sites with sparsely located devices must be inspected. Time constraints, the labor-intensive nature of inspection tasks, device accessibility constraints, and possible exposure to harmful contaminants in runoff are critical barriers to manual field inspections.

sUAS data collection offers numerous opportunities for ESCD inspection, especially when field visits are unsafe and manual inspection is economically prohibitive. While the majority of literature studies on ESCD inspection have focused on monitoring the effectiveness of control measures through the inspection of site terrain (Carabassa et al. 2021, Olivetti et al. 2020, Young et al. 2021) and on developing installation guides for different ESCDs (Cooke et al. 2015, Kastridis et al. 2022), few studies have investigated the use of automatic ESCD feature extraction to assess the overall condition of these devices. For example, Kazaz et al. (2021) trained the Single-Shot Multibox Detector model, a deep learning model capable of object detection and other vision-related tasks, for the detection of different ESCDs in orthophotos processed from sUAS images.

However, detection alone is insufficient for effective ESCD monitoring. Subsequent and more critical steps are required that involve detailed evaluation of device condition and performance. In this study, we developed a seamless and rapid prototype data processing pipeline that proceeds from data collection through data visualization, enabling inspection personnel to adequately inspect ESCDs in a timely manner using a method similar to that used for field inspections. We thus view device detection as an initial step in the monitoring workflow; detection may be performed as demonstrated by Kazaz et al. (2021) or manually through visual inspection of processed orthophotos.

Since replicating the traditional manual inspection process using remote assessment tools also requires an expedited transformation from the data collection and processing stage to final visualization, we developed a framework for the practical adoption of sUAS for monitoring ESCDs. Framework development involved the following tasks:

- Development of a prototype workflow for sUAS data collection and processing
- Sharing and presentation of processed red/green/blue (RGB) images and multispectral orthophotos through a low-latency data-viewing application
- Remote monitoring of devices through an advanced feature extraction workflow and multiview assessment
- Automatic extraction of features such as vegetation growth, rock coverage, side profiles, and upstream and downstream elevations from processed sUAS data using prototype tools

Goals and Objectives

The overall objective of this pilot study was to evaluate the application/adoption of sUAS technology for monitoring ESCDs. To achieve this objective, the following goals were established:

- Develop a prototype workflow for rapid sUAS data collection and data visualization
- Develop prototype feature extraction frameworks for the assessment of ESCD condition

STUDY AREA

The research team contacted Iowa Department of Transportation (Iowa DOT) staff on June 27, 2025, to obtain recommendations for construction sites featuring ESCDs. The Iowa DOT recommended two active grading project sites (Site 1: 41.065467, -91.176714; Site 2: 41.012754, -91.174138) along Highway 61 near eastern Mediapolis in Des Moines County, Iowa. The research team first visited the grading project sites in Mediapolis (hereafter called the Mediapolis sites) on July 11, 2025, for a preliminary study. As is typical during preliminary site visits, we noted several site variables, including construction traffic volume, the presence of overhead electrical cables, and the presence of ESCDs. The Iowa State University (ISU) and Michigan Tech Research Institute (MTRI) research team visited the sites on July 16, 2025, to collect comprehensive data using our sUAS platforms. As shown in Figure 1, members of the Technical Advisory Committee (TAC), including Melissa Serio and Wes Musgrove, among others, also joined us on the sites to explain in detail the ESCDs' performance and current inspection techniques, along with expectations for the sUAS survey.



Figure 1. Iowa DOT representative with the ISU and MTRI research team

The research team visited the Mediapolis sites again on August 27, 2025, with the primary goal of collecting new data and comparing the current condition of the ESCDs with their condition as recorded in the previous month's data. However, a significant amount of construction work, including the removal and replacement of the ESCDs, had already been completed. For example, most silt fences had been completely removed, and some rock check dams had been replaced with wattles. Therefore, no data were collected during the second visit.

We notified the TAC members about the new development on August 29, 2025, and received a new site recommendation on September 2, 2025. The second recommended site was a grading project site (41.315838, -92.699494) connecting 235th Street to Highway 63 in Oskaloosa, Mahaska County, Iowa (hereafter called the Oskaloosa site). As had been done at the Mediapolis sites, the team conducted a preliminary visit to the Oskaloosa site on September 10, 2025, before the final data collection effort by the MTRI team on September 23, 2025.

Overviews of the site locations and maps of both the Mediapolis and Oskaloosa sites are provided in Figure 2 and Figure 3, respectively. Figure 4 and Figure 5 show close-up views of some of the devices at Mediapolis Sites 1 and 2, respectively, while Figure 6 shows close-up views of some of the devices at the Oskaloosa site.

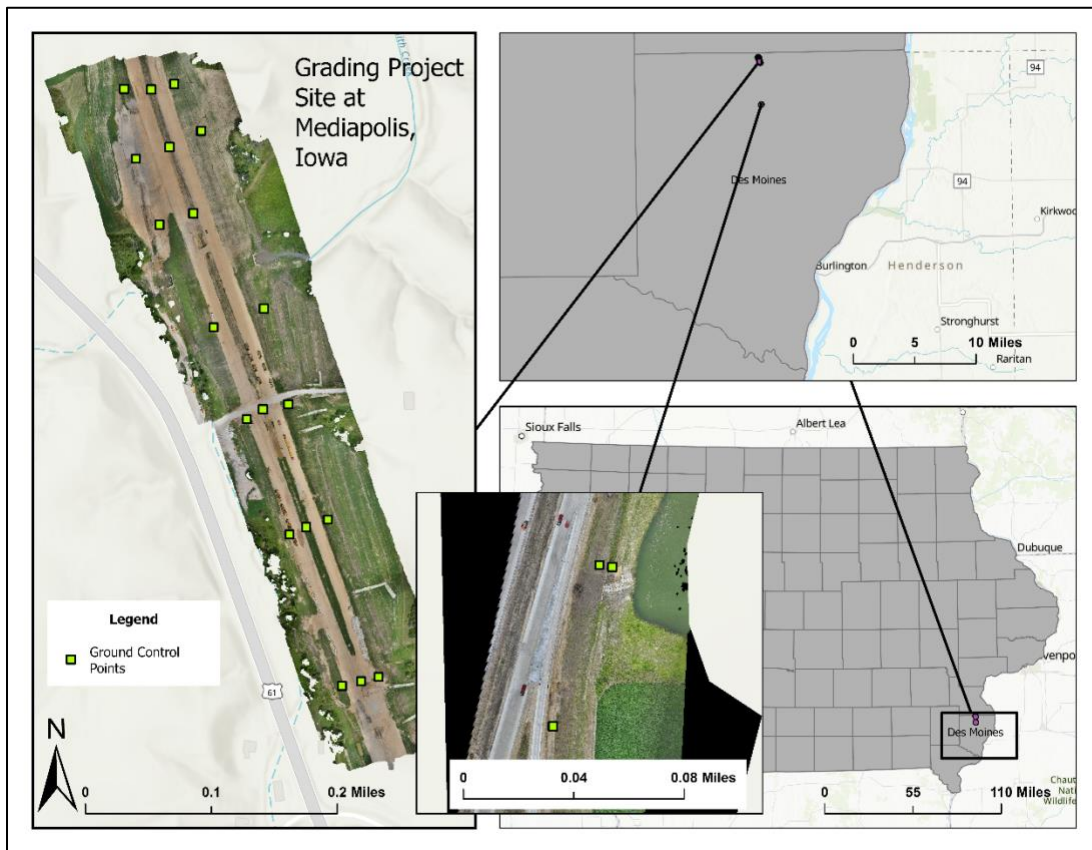


Figure 2. Grading project site in Mediapolis, Iowa

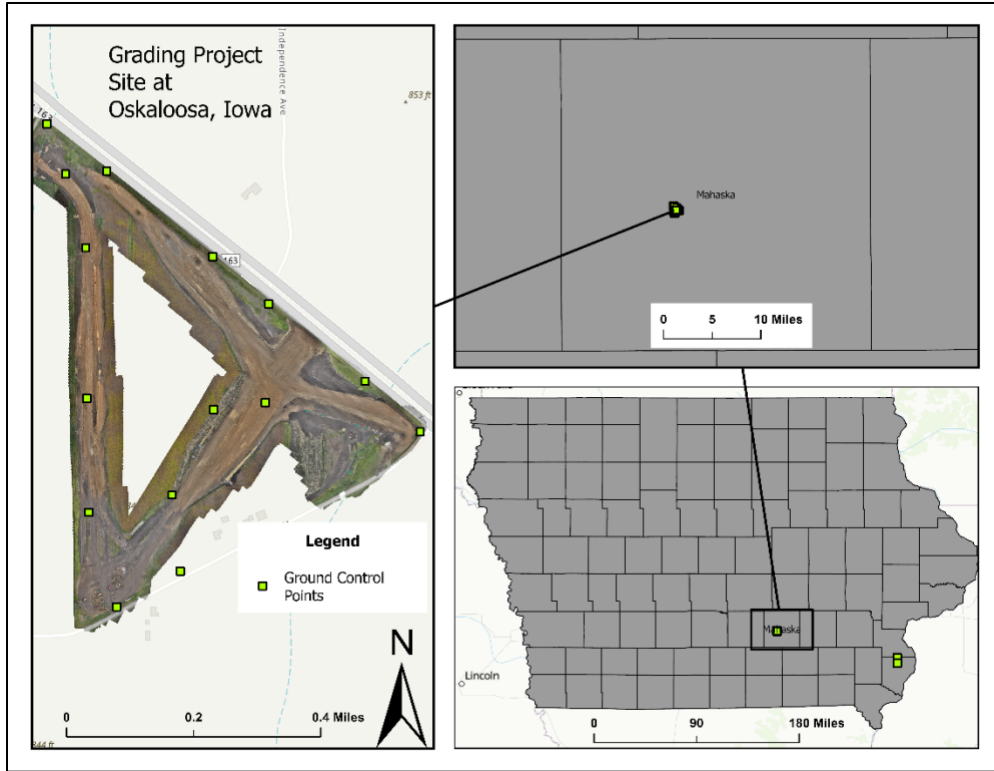


Figure 3. Grading project site in Oskaloosa, Iowa



Figure 4. Erosion and sediment control devices at Mediapolis Site 1, including silt fences and a check dam



Figure 5. Erosion and sediment control devices at Mediapolis Site 2, including wattles, a reseeded slope, and a check dam



Figure 6. Erosion and sediment control devices at the Oskaloosa site, including wattles

DATA COLLECTION, PROCESSING, AND VISUALIZATION

sUAS data collection and processing entail meticulous procedures that must be strictly adhered to for seamless operation and the delivery of desired results. Given that the Iowa DOT conducts weekly field inspections of ESCDs, it was imperative to produce not only a seamless data processing pipeline but also an expedited workflow that would deliver processed data within 24 to 48 hours. We therefore sought to identify the critical features that would support expedited and seamless sUAS operations, enabling the delivery of processed data at the right time for remote assessment and device condition monitoring. Figure 7 illustrates the prototype workflow for transitioning data from collection to visualization, and the subsequent sections in this chapter discuss the aspects of this workflow in detail.

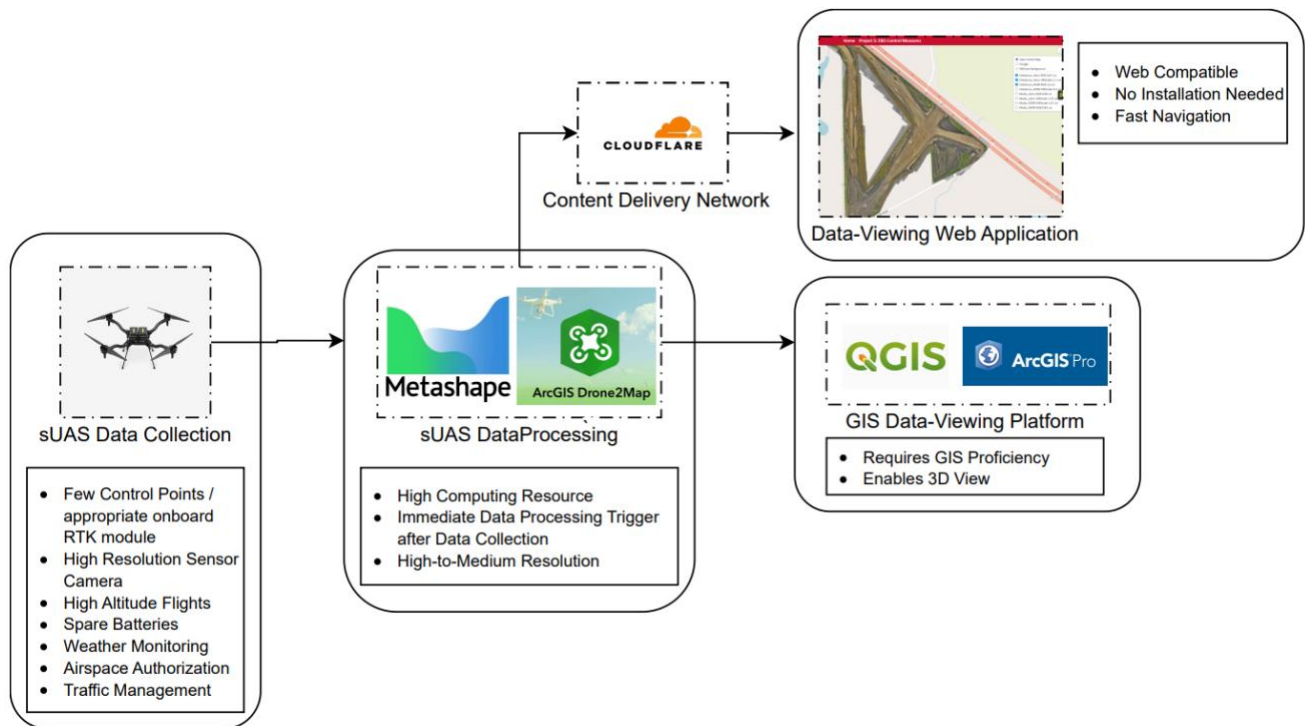


Figure 7. Data pipeline from collection to visualization

sUAS Data Collection

Data collection planning began with a discussion of requirements with TAC members. As mentioned earlier, the research team collected sUAS data from the Mediapolis sites on July 11, 2025, and from the Oskaloosa site on September 23, 2025. The sUAS data were collected from the Mediapolis and Oskaloosa sites using three different sUAS platforms: a Freefly Astro equipped with a Sony LR1 61 MP camera, a DJI Mavic 2 Enterprise Advanced (M2EA) equipped with 48 MP quad-bayer RGB camera and a 640x512 thermal camera, and a DJI Mavic 3 Multispectral (M3M) equipped with 5 MP multispectral cameras. Flight details are provided in Table 1.

Table 1. Summary of visited sites and deployed sUAS platforms

Target Area	Platform	Payload	Flight AGL (m)	No. of Images	Output Resolution (mm)	
					RGB/DEM	Other
Mediapolis Site 1	Freefly Astro	Sony LR1 61 MP	61.0	2672	6.8/13.5	
	M3M	20 MP RGB and 5 MP MS	30.5	2480	8.3/16.6	14.5 (MS)
	M2EA	640x512 thermal	91.4	1082		127 (TH)
Mediapolis Site 2	M3M	20 MP RGB and 5 MP MS	30.5	132	10.5/31.8	
	M2EA	640x512 thermal	15.2	459	28	
Oskaloosa	Freefly Astro	Sony LR1 61 MP	42.7	2676	6.7/26.8	
	M3M	20 MP RGB and 5 MP MS	45.7	2122	15.8/63.2	20.3 (MS)
	M2EA	640x512 thermal	91.4	1584		120 (TH)

MP = megapixels, MS = multispectral, TH = thermal, AGL = above ground level, DEM = digital elevation model

The research team followed standard safety and operating protocols to ensure safe and efficient data collection. Notable measures included, but were not limited to, the use of highly accurate ground control points (GCPs) such as Propeller Aeropoints, a dedicated visual spotter, flight paths that did not fly over people who were not part of the research team (including traffic), flights only during favorable operating conditions, and so on. As shown in Table 1, the research team took about 38 minutes to collect very high-resolution RGB data from the Mediapolis 1 site using the Freefly Astro at 61 m above ground level (AGL). Additional data were collected using the M3M at 30.5 m AGL. Thermal data were collected at 91.4 m AGL using the M2EA system’s thermal camera. At the Mediapolis 2 site, data were collected using the M2EA at 15.2 m AGL and the M3M at 30.4 m AGL. At the Oskaloosa site, the research team focused on collecting data using the Freefly Astro at 42.7 m AGL. Additional data were collected using the M3M at 45.7 m AGL and the M2EA at 91.4 m AGL.

Critical factors that must be adequately addressed during sUAS data collection include the following:

- Ground control points/real-time kinematics (RTK) module:** For sites with a large surface area, the placement and retrieval of GCPs may be challenging. While positional accuracy is crucial, especially when creating digital repositories that will be used for comparing data collected on different dates, selecting an optimal number of GCPs is essential to achieve consistent spatial accuracy and expedite sUAS data collection workflows. A practical approach is to place the GCPs at the corners of the site while ensuring that they are pliable for easy placement and retrieval. Drones with an onboard GPS RTK module also receive geopositional corrections from satellites, thereby reducing the number of GCPs required for data collection. Our workflow solely depended on the use of high-resolution GCP, and RTK technology was not used.

- **High-resolution sensor:** The achievable ground sampling distance depends on the resolution of the sensor on board the sUAS. A high-resolution camera enables a higher flight altitude, in turn resulting in a shorter required flight time. A 150 to 200 ft flight altitude (46 to 76 m) over a large area may yield high- to medium-resolution imagery, provided that a high-resolution sensor, such as a Sony LR1 61MP camera, is on board the sUAS.
- **Spare resources:** Proper planning to ensure that the resources required for flight operations are on hand is crucial to achieving a seamless sUAS data collection workflow. For example, because most sUAS batteries typically last only 20 to 30 minutes, supplies such as AC generators or DC batteries should be readily available for charging sUAS batteries immediately after depletion in order to reduce downtime during flight operations.
- **Weather monitoring:** Monitoring weather data is crucial because sUAS flight operations are best conducted in precipitation-free conditions with low to no wind gusts. Abrupt changes in weather conditions are not uncommon, and if weather conditions turn unfavorable, flight operations must be suspended for safety. Continuous tracking of weather conditions is advised, particularly in the early hours of the data collection date, because doing so typically reveals the most likely weather events of the day.
- **Airspace approval and other authorizations:** Any sUAS flight conducted within controlled airspace requires prior authorization from the Federal Aviation Administration (FAA). Operators must account for potential processing delays because approval timelines may be affected by operational constraints or unforeseen circumstances. Consequently, flight planning should begin well in advance of the anticipated mission date. Operators must be fully familiar with the project site, land traffic conditions, and the corresponding airspace classification to determine whether authorization is required. Obtaining airspace permission requires using the FAA-approved Low Altitude Authorization and Notification Capability (LAANC) website or mobile app. Because the operations conducted for this study did not fall under the recreational category, at least one Remote Pilot in Command was required to hold a valid Part 107 certification issued by the FAA, and this person was to be held responsible for the safe conduct of the flight operation. The use of visual observers is also strongly recommended to maintain a continuous visual line of sight with the aircraft, monitor the surrounding airspace for potential conflicts with manned aircraft, and ensure separation from obstacles and other hazards throughout the flight.

sUAS Data Processing

The data collected from the Mediapolis and Oskaloosa sites were processed using Agisoft Metashape, a widely used close-range photogrammetry software package that includes distributed processing capabilities. Three computers equipped with Intel Xeon processors, 128 to 192 GB of ECC RAM, and NVIDIA QUADRO RTX graphics cards were used for this processing. Each dataset was imported into Agisoft Metashape, where image alignment was performed. High-resolution GCP data were collected and processed using the Propeller AeroPoint platform, then imported into Agisoft Metashape to correct the positions of the captured images. The research team used 22 GCPs at the Mediapolis sites and 14 at the

Oskaloosa site. The RGB data from the Freelyfly Astro and M3M systems were used to generate RGB orthomosaics and digital elevation models (DEMs) using Agisoft Metashape. The DEMs were later processed to create hillshade models. Additionally, multispectral data from the M3M and stereo thermal data from the M2EA were used to generate four-band multispectral orthomosaics and thermal orthomosaics, respectively. The resolution of each dataset is provided in Table 1.

sUAS Data Visualization

Rapid access to sUAS data is essential for ESCD monitoring and performance evaluation, particularly following precipitation events. To demonstrate the feasibility of timely data delivery, the research team developed a prototype online data sharing platform that hosts processed RGB orthophotos and DEM files. The web portal was built using the Leaflet application framework, which enables dynamic data retrieval from a public server. To improve performance and loading efficiency, the orthophotos were divided into smaller image tiles and hosted on a Cloudflare server, allowing the portal to seamlessly fetch and display the data. Members of the MTRI research team uploaded similar datasets to MTRI’s existing server infrastructure, and all related drone data were also made available for viewing and access through the platform. Figure 8 and Figure 9 are screenshots from <https://prosperiastate.github.io/> and https://apps2.mtri.org/iowa_dot_viewer/home, respectively.



Figure 8. Web-based data viewing platform (Iowa State University version)

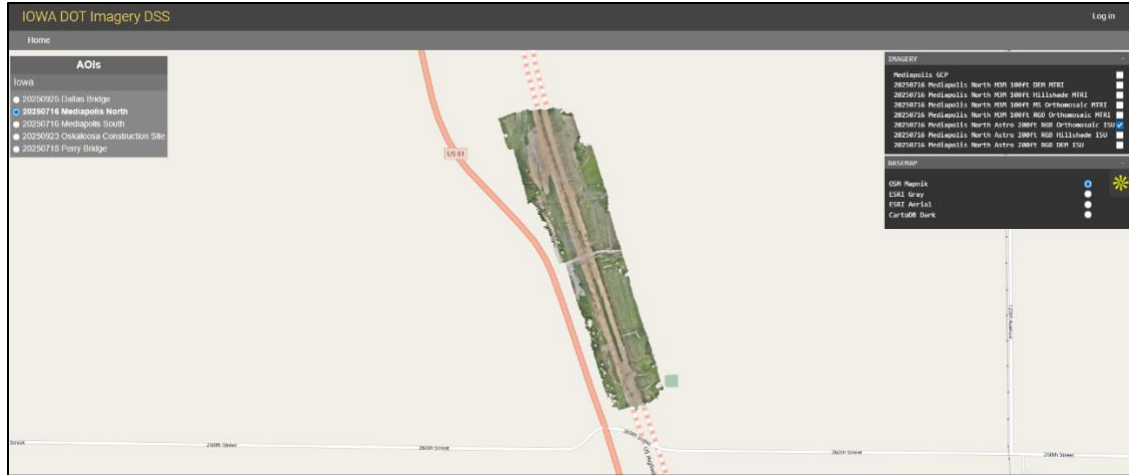


Figure 9. Web-based data viewing platform (MTRI version)

DEVICE MONITORING

Vegetation

Vegetation, used as an erosion and sediment control mechanism, is a biological product that mitigates the impact of sediment dislodgement and erosion on construction sites (Mahmud 2021, Osterkamp et al. 2012). While some vegetation functions as a canopy, shielding exposed soil surfaces from the direct impact of runoff that mobilizes sediment (Puigdefábregas 2005, Zuazo and Pleguezuelo 2009), other vegetation types contribute to soil stabilization by reinforcing the topsoil through interconnected root systems (Masi et al. 2021, Zhang et al. 2024). Consequently, since vegetative measures often serve as the primary ESCD when deployed, monitoring vegetation growth is critical.

While manual visual inspection is subjective, often inaccurate, and difficult to perform in hard-to-reach and sparsely vegetated areas, drone sensing offers very accurate and quantitative measurements and can inspect areas far beyond the reach of a human inspector. Previous studies have developed objective metrics to estimate vegetation greenness (Bannari et al. 1995). According to Xue and Su (2017). However, the complexities of different light-spectra combinations, instrumentation platforms, and image bands and resolutions have precluded a unified mathematical expression that defines all vegetative indices, so an objective metric is dependent on the collected data.

The M3M sUAS deployed for our data collection captures reflectance in the green, red, red edge, and near-infrared (NIR) bands. The system's multispectral camera collects data at narrower spectral bandwidths in the green and red bands than normal RGB cameras. The wavelength centers and bandwidth sizes captured by the camera are as follows: green: 560 nm \pm 16 nm; red: 650 nm \pm 16 nm; red edge: 730 nm \pm 16 nm; and near-infrared: 860 nm \pm 26 nm. These bands allow the use of objective metrics that require information on any of the four available bands, but it is essential to note that accurate interpretation of the metrics, along with awareness of the metrics' shortcomings, is critical when adopting them for qualitative and quantitative assessment of vegetation growth. For example, the Normalized Difference Vegetation Index (NDVI) is an effective metric for expressing vegetation status and attributes as reflected in spectral imagery (Huang et al. 2021). With NDVI values ranging from -1 to 1, negative values are typically associated with water bodies; values close to 0 are associated with rocks, sand, and concrete surfaces; and positive values are associated with the presence of living vegetation. Another popular index is the Soil-Adjusted Vegetation Index (SAVI). The SAVI was established to improve the NDVI's sensitivity to the soil background, where L in its formula represents the soil conditioning index, which helps tune this sensitivity (Xue and Su 2017). The L value ranges from 0 to 1, with the selected L value determined by environmental conditions. For example, values close to 1 signify that the soil background does not affect the extraction of the vegetation information. The SAVI approaches the NDVI as L approaches 0. Another metric—the Modified Soil-Adjusted Vegetation Index (MSAVI)—does not rely on the soil line principle and has a simpler algorithm. Similar to the NDVI, higher positive values in the SAVI and MSAVI also indicate vegetation growth. Equations (1) through (3) provide mathematical expressions of the NDVI, SAVI and MSAVI, respectively.

$$NDVI = \frac{NIR-RED}{NIR+RED} \quad (1)$$

$$SAVI = \frac{NIR-RED}{NIR+RED+L} (1 + L) \quad (2)$$

$$MSAVI = \frac{2NIR+1-\sqrt{(2NIR+1)^2-8(NIR-RED)}}{2} \quad (3)$$

We developed a proof-of-concept toolbox in ArcGIS Pro capable of extracting the required image bands from the raster files for the calculation of each pixel’s vegetation index, with users expected to know what each band number represents. A screenshot of the toolbox is shown in Figure 10, with bands 2 and 4 representing the red and near-infrared bands, respectively. Since the end product of analysis is to binarize each pixel value as either vegetation or non-vegetation, users are expected to provide a class threshold boundary (in the screenshot, a value of 0.3 has been provided), above which index pixels are classified as vegetation and below which pixels are classified as not vegetation. We also integrated the NDVI, SAVI, and MSAVI formulae into the code, allowing users to select one of the three expressions per analysis run.

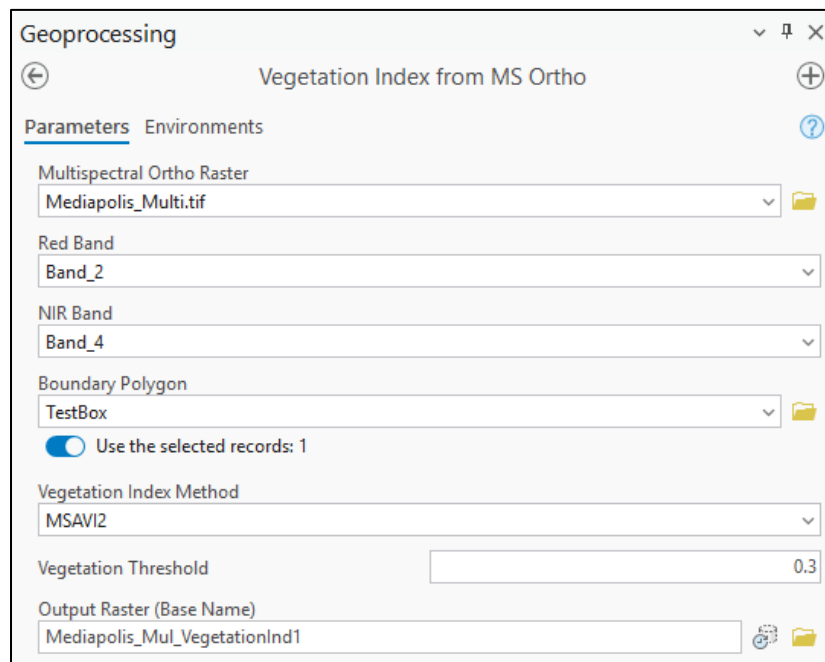


Figure 10. ArcGIS Pro proof-of-concept toolbox for automatic vegetation index estimations

Since Mediapolis Site 1 had vegetation installed on the slopes for erosion and sediment control, we tested the automatic analysis workflow using processed multispectral ortho-imagery from that site. Figure 11, Figure 12, Figure 13, and Figure 14 show the results of the data analysis for the multispectral image shown in the middle of each figure, with the left image showing the MSAVI results ranging from -1 to +1 and the right image showing the pixels classified as vegetation or non-vegetation based on the chosen threshold. It should be noted that users should carefully choose vegetation thresholds to obtain accurate vegetation cover calculations, as

several factors such as grass health, season of data collection, sun angle, soil moisture content, soil background, and atmospheric conditions can influence the appropriate threshold value.

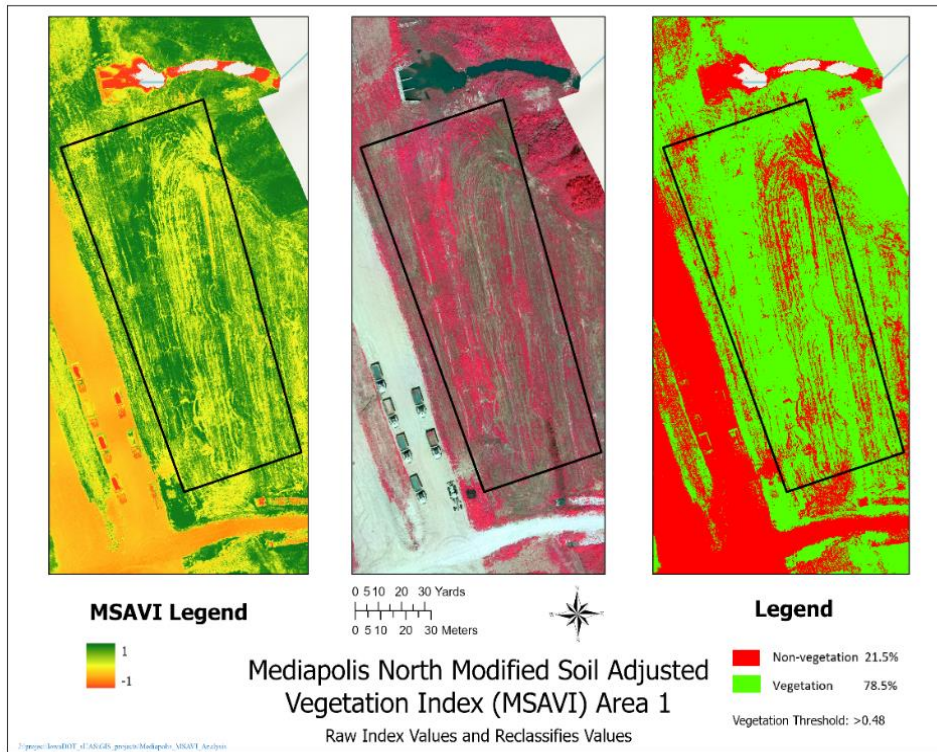


Figure 11. Mediapolis Site 1 MSAVI results for demarcated area 1

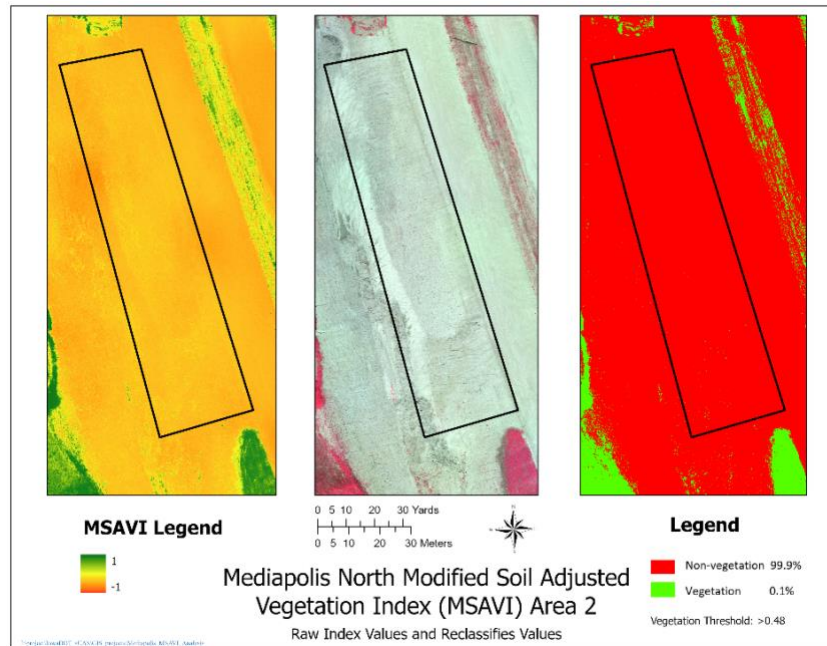


Figure 12. Mediapolis Site 1 MSAVI results for demarcated area 2

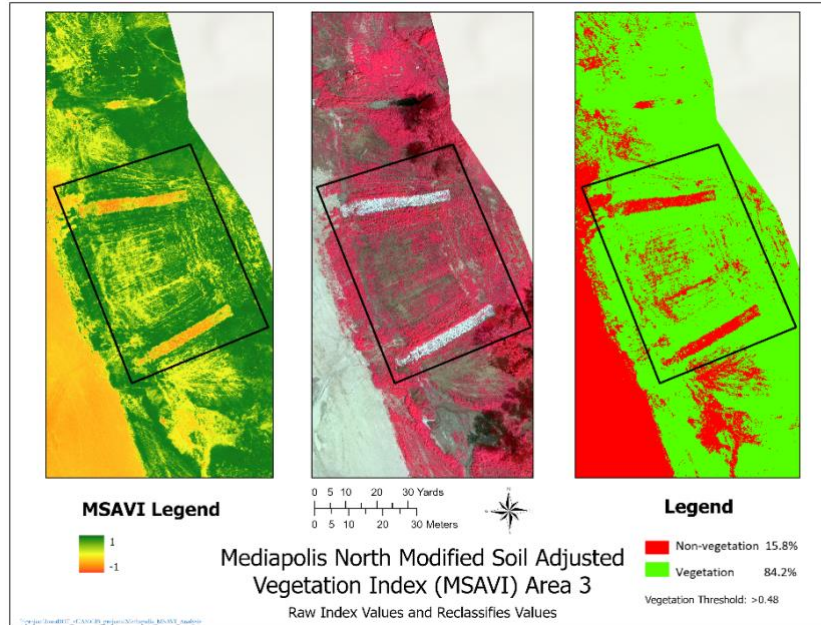


Figure 13. Mediapolis Site 1 MSAVI results for demarcated area 3

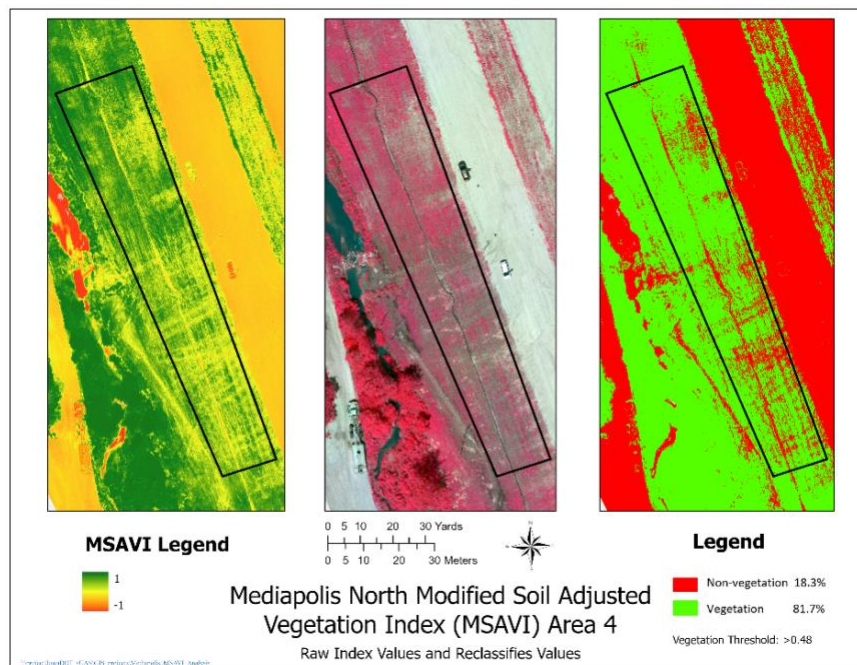


Figure 14. Mediapolis Site 1 MSAVI results for demarcated area 4

Rock Check Dams

Rock check dams are ESCD structures installed mainly to impede the flow energy of sediment-carrying runoff water. Check dams were installed in ditches leading to free-flowing streams at both the Oskaloosa and Mediapolis sites. While remote visual sensing of these check dams

provides information on rock conditions and an assessment of upstream/downstream conditions, one may be interested in a quantitative and qualitative assessment that maps image features to the overall condition of the rock check dams. As evidenced in published literature, the majority of studies related to rock check dams have focused on investigating the efficacy of such devices in controlling erosion and sediment under different conditions (Castillo et al. 2007, Margiorou et al. 2022, Theofanidis et al. 2025). In this study, we focused on how to assess the current conditions of the check dams at the study sites and develop innovative approaches to inform maintenance and asset management decisions.

Analysis of check dam conditions from processed sUAS data involves two tasks: (1) assessment of upstream and downstream conditions with respect to the check dam and (2) assessment of rock concentrations within the bounded check dam area. While the former assessment leverages DEM data, the latter uses the automatic workflow of an unsupervised machine learning algorithm to filter out rock pixels in the image and leverages other algorithms to count the detected rock pixels and evaluate the overall area covered by rock and non-rock materials.

The relative upstream and downstream elevations across a check dam area provide a practical indication of the available headroom for accommodating future sediment accumulation. A larger elevation difference generally suggests greater remaining storage capacity, while a smaller difference may indicate that the structure is approaching sediment saturation. To automate this assessment, the project team developed a proof-of-concept programmatic workflow in ArcGIS Pro using a custom toolbox. In this workflow, users first identify the location of a check dam by drawing a polygon feature in ArcGIS Pro over the dam to serve as an input parameter to the toolbox. Based on the geometry of this feature, the longer side is mathematically identified and assumed to represent the dam alignment. Using this orientation, a new polygon is generated that preserves the angular orientation of the original but extends outward on both sides of the longer edge. These extensions are designed to capture the upstream and downstream portions of the channel adjacent to the check dam. An important simplifying assumption is introduced at this stage. The stream flow direction on either side of the dam is assumed to be perfectly orthogonal to the longer side of the quadrilateral feature. While this assumption may not hold in all natural settings, it provides a consistent geometric basis for automating the analysis and is reasonable for relatively straight channel segments near check dams. After polygon generation, a series of profile-guiding lines is created across the extended feature. These lines are used to sample elevation values from a DEM raster file input by the user. The sampled elevation points are then spatially grouped into three distinct sections: upstream reach, check dam location, and downstream reach. Finally, elevation profiles from these three sections are extracted and plotted against one another to provide a visual and quantitative representation of the channel condition and sediment accumulation pattern relative to the check dam, enabling a rapid assessment of its current performance and remaining sediment storage potential.

Using the prototype toolbox shown in Figure 15, users provide raster files for the DEM, orthophoto, and multispectral imagery. Under the hood, the program first captures the input polygon, extends its longer edges, and adds lines across each section to ensure accurate elevation sampling, as shown in Figure 16. The clipped rasters are used for image processing to detect rock coverage, while the sampled elevations from upstream, check dam, and downstream sections are used to profile the cross-elevation of the device.

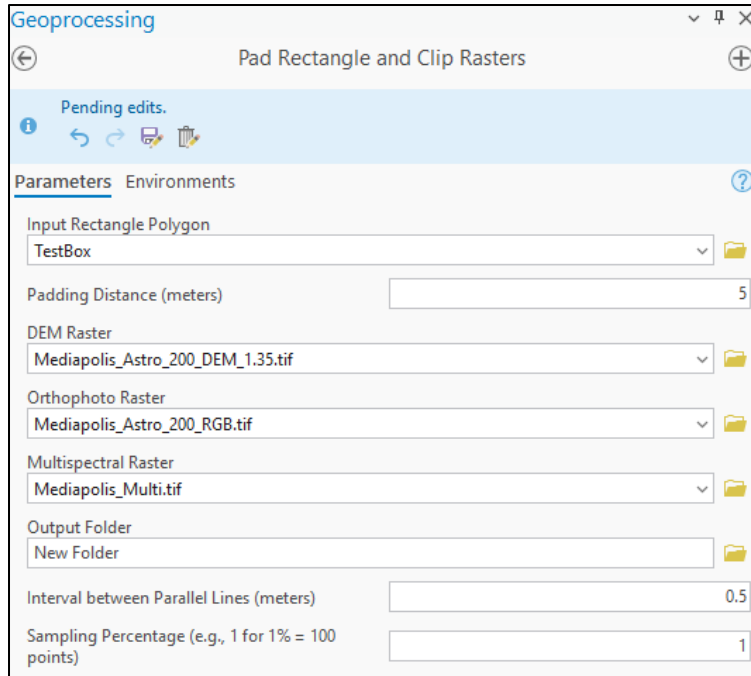


Figure 15. Screenshot of ArcGIS Pro proof-of-concept toolbox for raster clipping and elevation analysis of a rock check dam

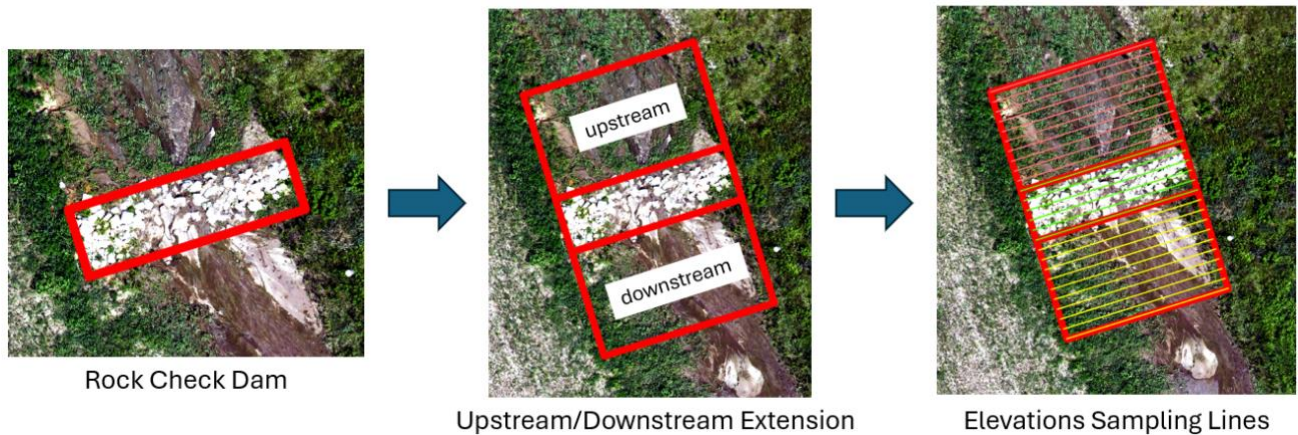


Figure 16. Flowchart showing line development for elevation sampling

For the check dam at Mediapolis Site 1, shown in Figure 16, we processed the elevation plot and generated front and side elevations using the developed toolbox, as shown in Figure 17 and Figure 18, respectively. While the profile of a well-performing check dam would typically be above both the upstream and downstream sections, as shown in the bounded region of Figure 17, the check dam profile line in this case, represented in green, is below the upstream section and almost at the same level as the downstream section. Intuitively, this analysis provides a quantitative overview of sediment and vegetation overflows within the check dam region.

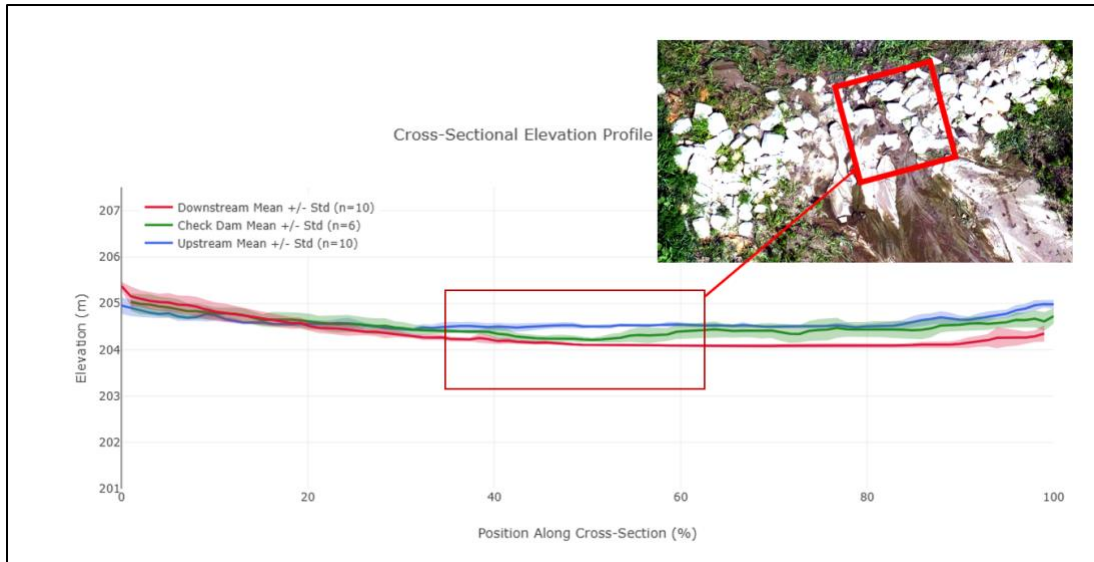


Figure 17. Front elevation of a check dam, upstream and downstream

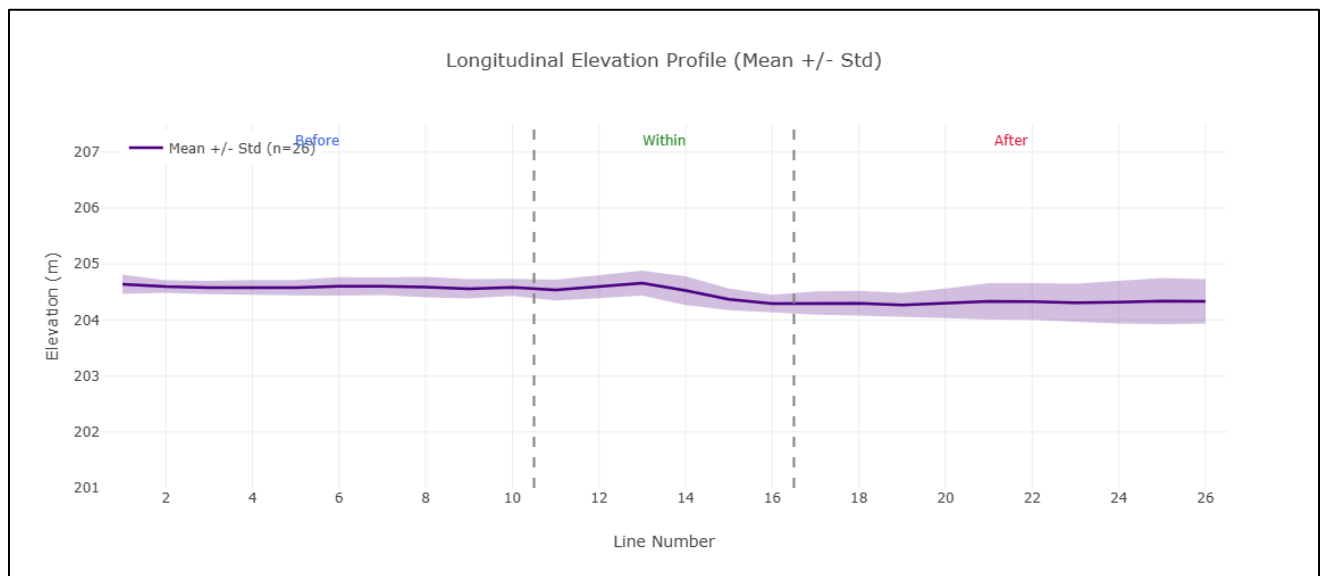


Figure 18. Side elevation of a check dam, upstream and downstream

From these elevation plots, which show both mean and standard deviation, one can quantify the condition of the check dam and make informed decisions about maintenance and the dam's reliability for mitigating future runoff events. We selected other check dams at both the Oskaloosa and Mediapolis sites and added their profile results (Figure 19 and Figure 20).

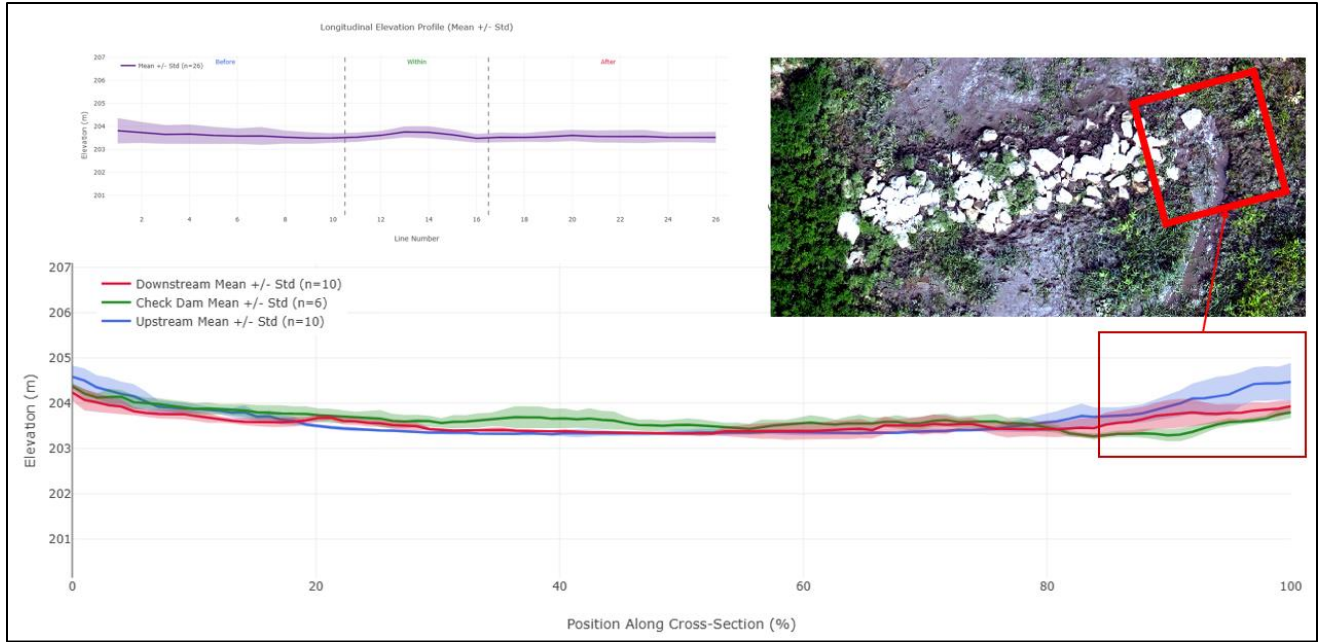


Figure 19. Front and side elevations of a check dam at Mediapolis Site 1, upstream and downstream

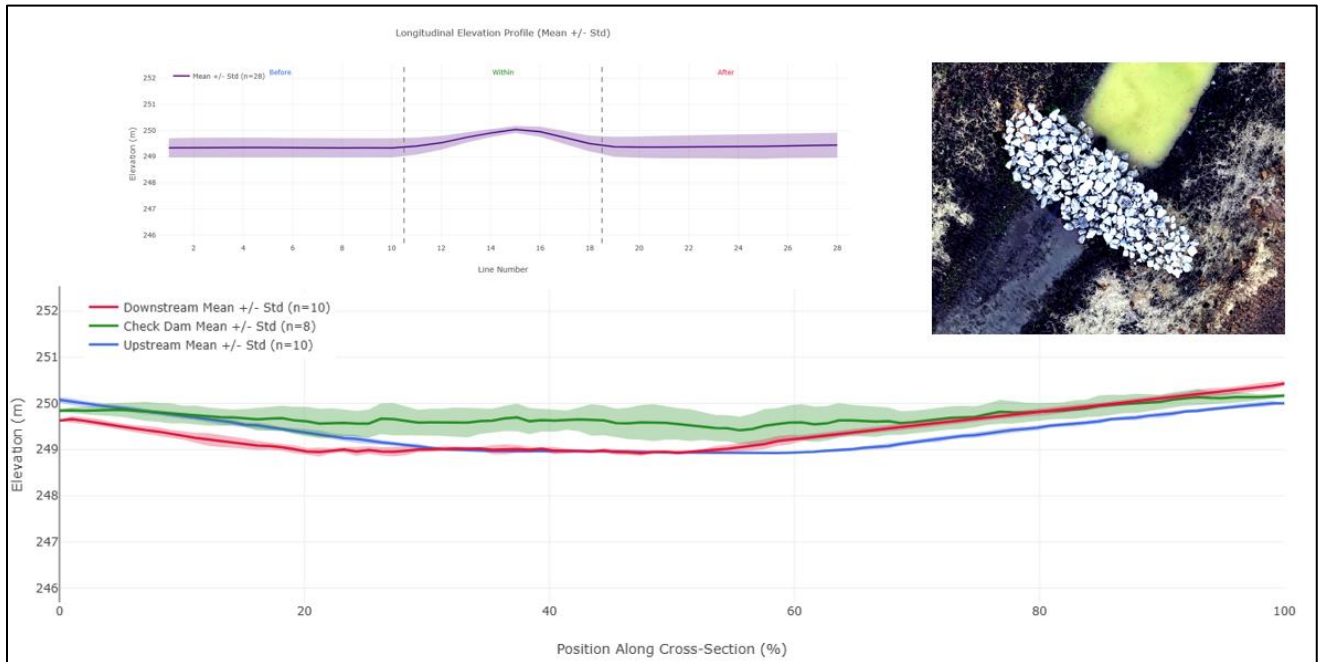


Figure 20. Front and side elevations of a check dam at the Oskaloosa site, upstream and downstream

Estimating rock coverage within the demarcated area of the rock check dam adds an extra layer of information that can be used to assess the overall condition of the dam. Leveraging all available bands from the orthophoto and multispectral imagery, we automatically segmented the

cropped image into its components and selected a filter that extracts only rock features. We adopted this automated rock analysis approach because it is challenging to manually select a binary threshold for segmenting rocks in images. Since varying light intensities, coupled with sediment and water overflows, make manual segmentation difficult, we passed the already cropped raster files from the initial DEM analysis toolbox to a K-means clustering algorithm, a machine learning algorithm that automatically groups data points with similar attributes (in most cases, points at a close spatial distance). Thus, pixels with numerical attribute values for each color band that indicated similar features in the image were grouped. Using this approach, one can segment rocky, wet sediment, dry sediment, grass, and other non-rock features in an image.

As illustrated in Figure 21, the entire rock check dam section was segmented into three categories: rock, non-rock, and background. In this analysis, cluster 1 corresponds to the rock features that were later passed to the OpenCV contour algorithm for further analysis. The resulting contour is shown in the bottom image in the figure. Using this method, one can estimate the percentages of rock and non-rock coverage in a processed sUAS image.

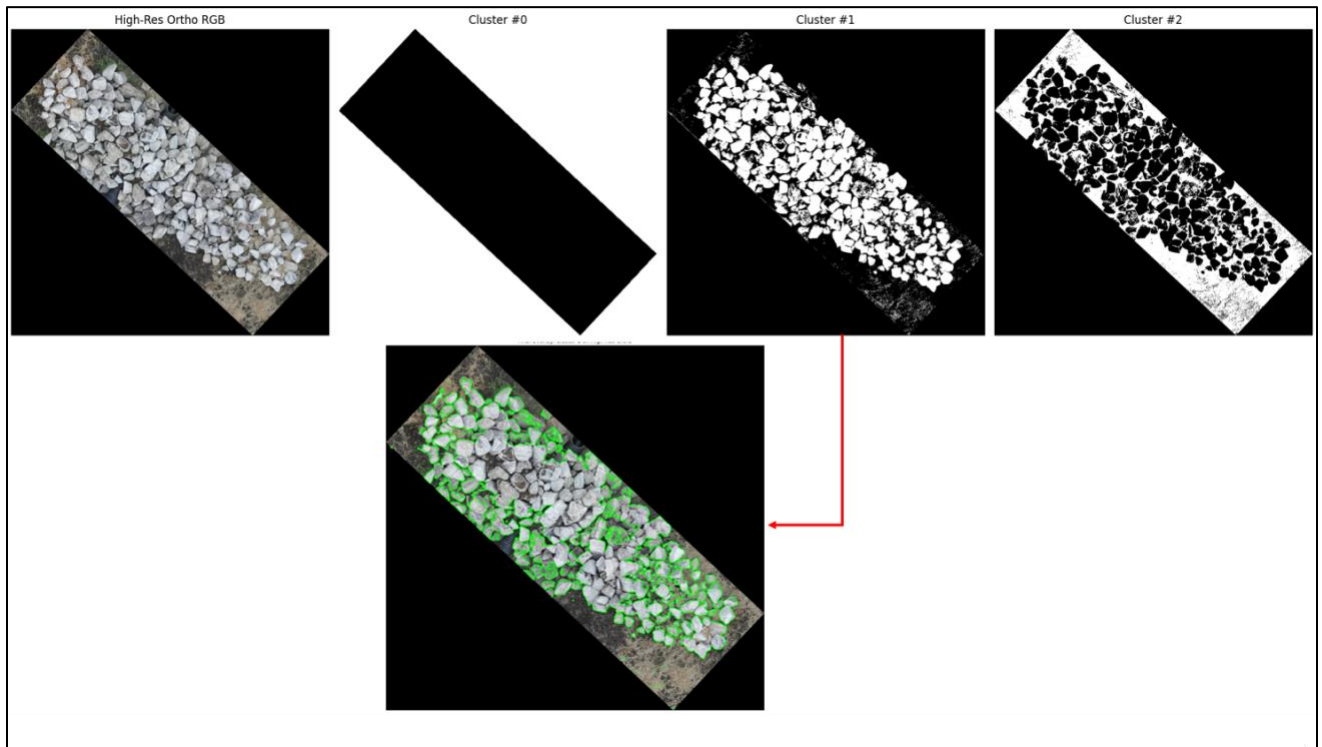


Figure 21. Automatic segmentation of rock check dam images using K-means clustering

Silt Fences

Silt fence devices, typically installed in ditches and along cut slopes, are commonly used for erosion control. In our study, we sought to determine how processed sUAS data can enable remote assessment of the condition of these devices. Similar to the devices discussed above, the majority of literature on silt fences has focused on material selection (Bugg et al. 2017, Risse et

al. 2008), installation techniques (Liu et al. 2021, Yeri et al. 2012), and their efficiency in controlling sediment. To assess the overall condition of silt fence installations, we developed three frameworks that can be used jointly to provide a comprehensive, accurate assessment: (1) elevation profiling, (2) sediment accumulation assessment using a vegetation index, and (3) 3D viewing. We discuss each framework in detail in this section.

The elevation profiling method described here for silt fences is similar to that used for check dams, in that DEM data are sampled for each pixel and later used to develop an elevation profile of the identified section. However, unlike check dams, which typically are relatively short, silt fences are typically long and can run across the full length of a site. We simplified the profile analysis here to focus only on the points of interest relevant to silt fences. This profile analysis indicates how a silt fence device behaves with respect to its upstream and downstream areas and reveals a consistent pattern in good-performing silt fences and sediment-overloaded silt fences. While the former typically have enough headroom both upstream and downstream to retain sediment, the latter mostly have a flat profile, with the sediment on the upstream side almost at the same elevation as, if not above, the top of the silt fence. A drastic drop in elevation downstream of the fence further indicates that the fence is under significant upstream sediment pressure and could break without quick intervention. A broken silt fence would create a jagged profile with no clear elevation pattern either upstream or downstream.

We developed an automated profiling toolbox prototype in ArcGIS Pro that requires users to provide a line feature (an orthogonal line crossing the silt fence) and a DEM raster file to sample and plot elevation points along the line feature. Figure 22 shows a screenshot of the toolbox.

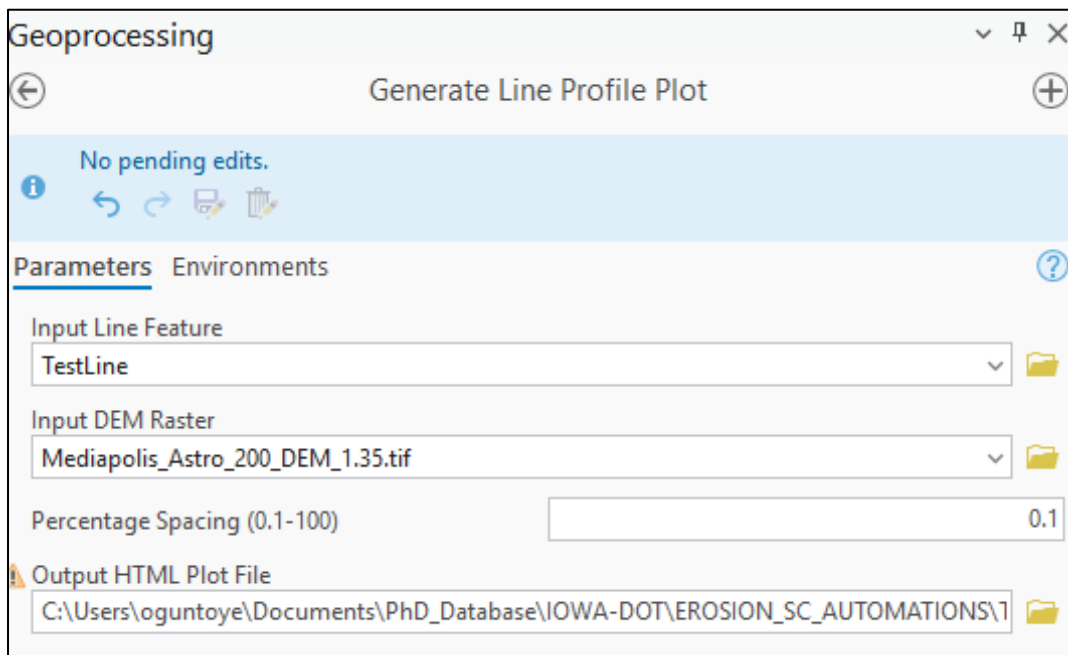


Figure 22. Screenshot of ArcGIS Pro proof-of-concept toolbox for profile plotting of silt fence areas

We performed profile analyses on selected silt fences, with the results shown in Figure 23, Figure 24, and Figure 25.



Figure 23. Plotted profile of a silt fence with accumulated sediment in the upstream section

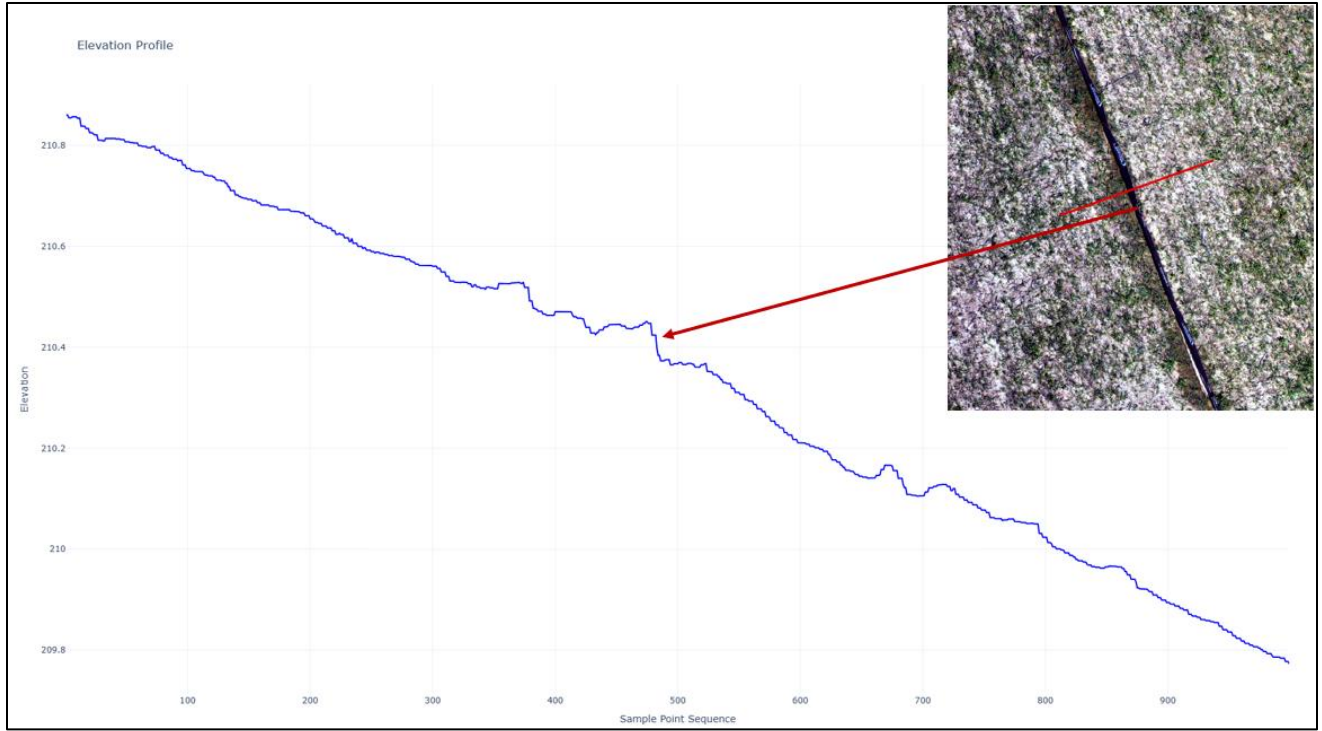


Figure 24. Plotted profile of a silt fence with no visible sediment in the upstream section

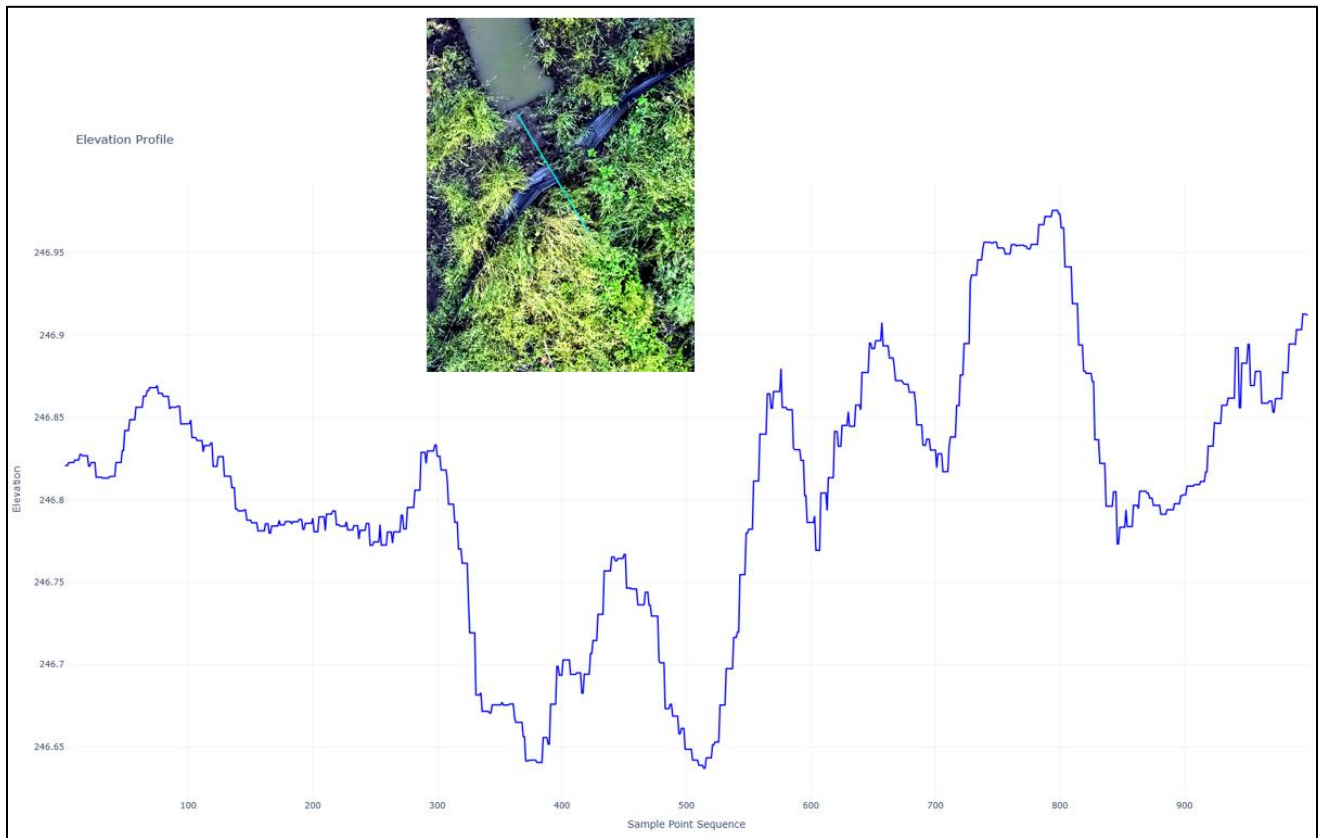


Figure 25. Plotted profile of a damaged silt fence

As stated earlier, the drastic drop shown in Figure 23 is indicative of sediment pressure on the silt fence, while the continuous slope profile shown in Figure 24 reflects a consistent profile with no visible concentrated sediment. The jagged profile in Figure 25 suggests possible abnormalities in or damage to the silt fence.

The second framework quantitatively analyzes the sedimented area on the upstream and downstream sides of a silt fence. We leveraged the proof-of-concept toolbox developed for the vegetation coverage analysis to quantify the percentage of vegetated and non-vegetated regions within a bounded area. For this task, however, we are more interested in how much non-vegetation is present, since that is indicative of sediment, water, and other non-vegetative features. Figure 26 illustrates the distribution of the greenness of vegetation and the redness of non-vegetation features around a silt fence. A close examination of the silt fence shows that the north end is experiencing greater sediment pressure. While the RGB orthophoto already visually shows the sediment accumulation, our toolbox is able to provide a quantitative assessment for better condition rating.

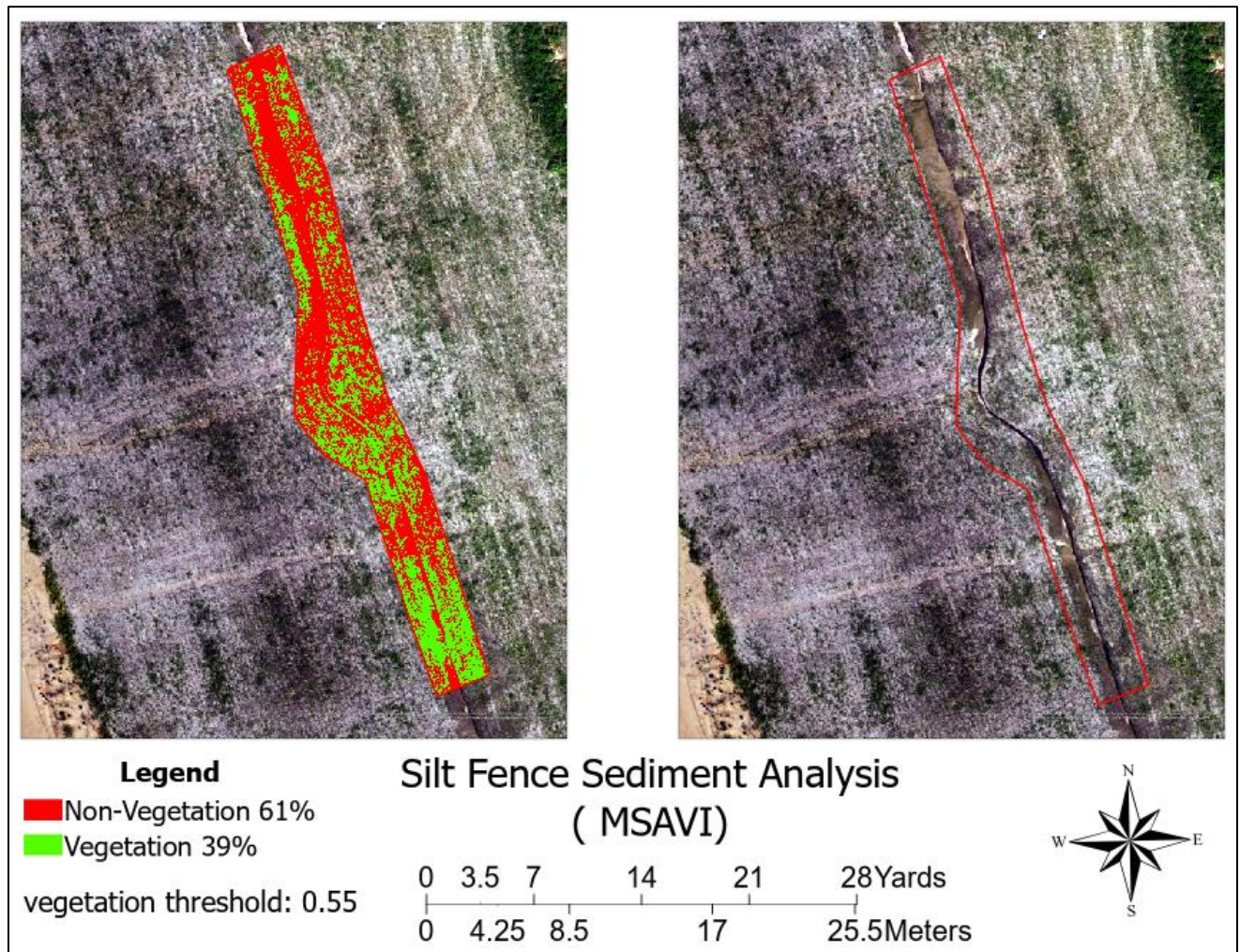


Figure 26. Vegetation index analysis of sediment accumulated near a silt fence

The third framework provides an additional layer of information through 3D viewing. While the orthophotos generated by sUAS are 2D, as shown in previous figures, ArcGIS Pro provides a feature that converts a 2D scene into a local or global scene, offering a 3D-like view for users to pan and zoom for further assessment. Figure 27 shows an overview of the global scenes from the Mediapolis and Oskaloosa sites, while Figure 28 provides a close-up of a silt fence at Mediapolis Site 1 from the global scene view.

It is crucial to note that because these scenes are not created based on the z-elevation from the processed DEM but rather from the natural terrain according to the default topography data in ArcGIS Pro, neither the elevation nor the terrain profile reflects the site's actual condition. The function of the 3D scenes is instead to allow for a multiview assessment of the ESCDs, which is essential for making a well-informed assessment of the overall condition of the devices.

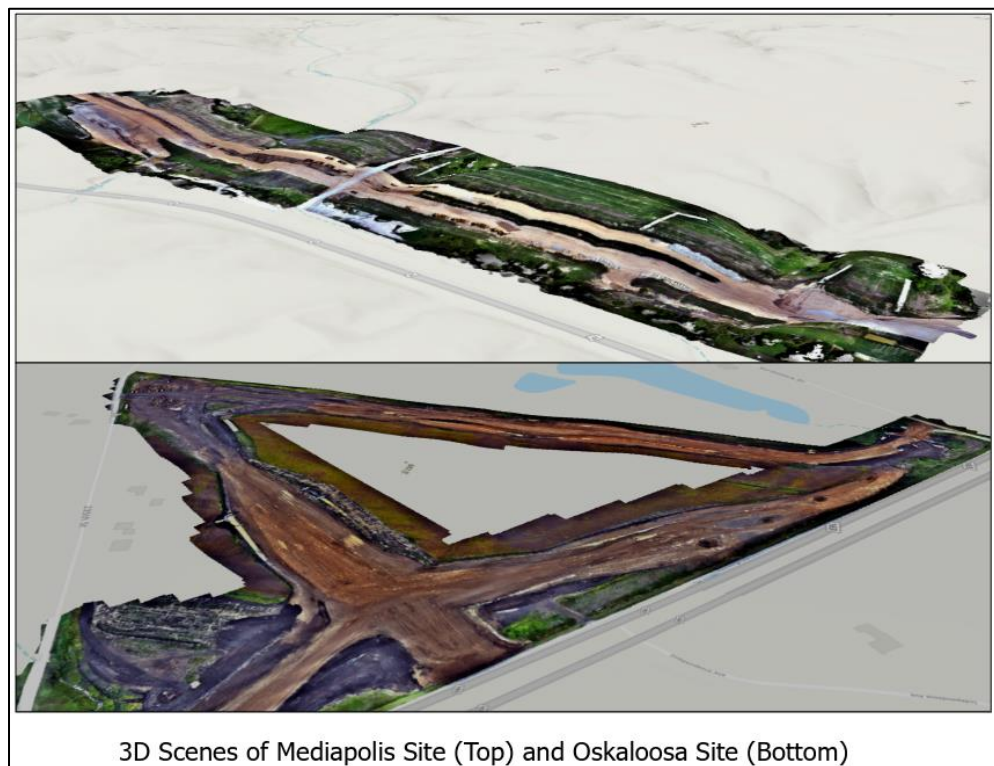


Figure 27. Overview of the global scenes from Mediapolis Site 1 and the Oskaloosa site

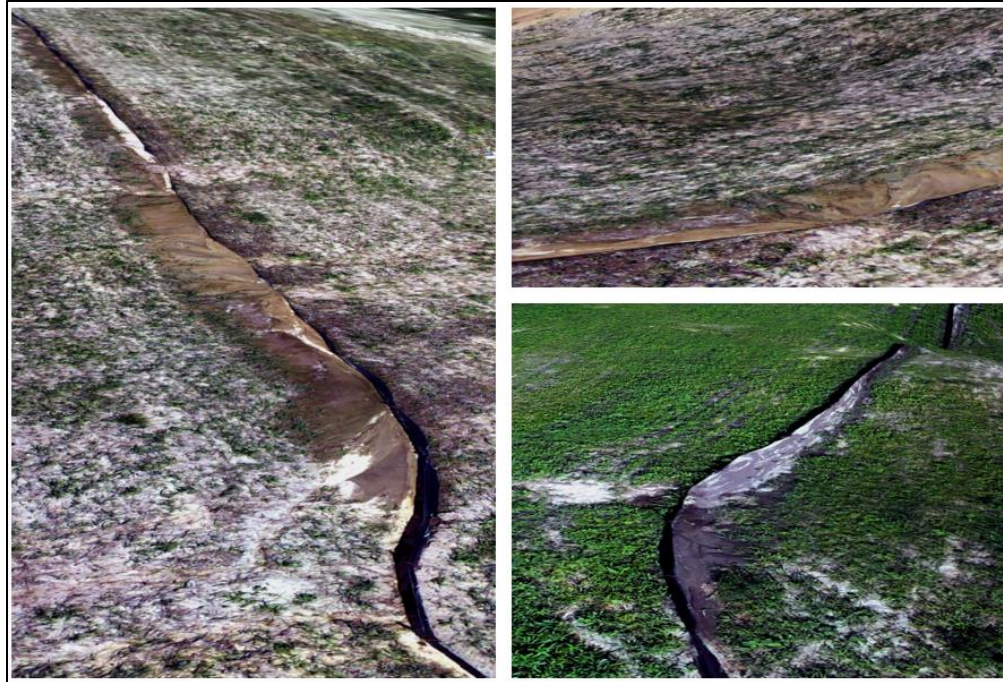


Figure 28. Close-up view of a silt fence at Mediapolis Site 1 from the global scene view

Combining the quantitative profile and sediment analyses with 3D viewing provides a comprehensive remote assessment technique for silt fence monitoring.

Wattles

A wattle is a linear, tube-like ESCD, typically stuffed with various materials such as excelsior fiber, wheat straw, wood chips, synthetic fiber, or other fillers (Whitman et al. 2021). Wattles are mostly installed on grading slopes and ditches to control runoff and impede the continuous transport of sediment. Assessing the condition of a wattle, as with other devices, is typically reserved for traditional inspection practices that check how it performs between the upstream and downstream sections. We therefore we investigated how collected and processed sUAS data can be used to monitor wattle condition. Similar to the proposed processes for silt fence condition assessment, wattle condition can be assessed based on (1) profile analysis and (2) 3D viewing.

Profile analysis quantifies the available headroom on the upstream side of a wattle and compares the top-level elevations of the downstream and upstream sections, from which one can determine whether sediment is overwhelming the wattle device. The proof-of-concept toolbox for conducting profile analyses of silt fences is applicable for wattles as well. Figure 29 illustrates how a wattle's profile can be plotted using the developed toolbox. Quantifying the level of sediment on the upstream and downstream sides of the wattle can help inform maintenance actions. For example, a profile plot showing upstream/downstream top elevations flush with that of the wattle would imply that the wattle needs to be replaced or that sediment needs to be excavated to accommodate more sediment from future precipitation runoff.

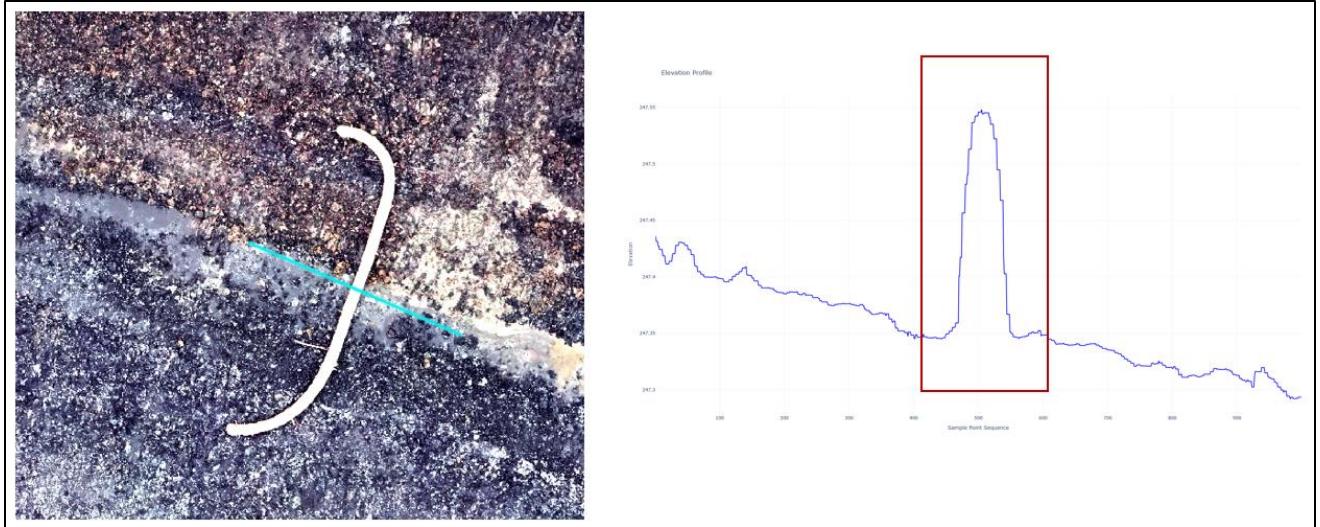


Figure 29. Wattle profile plot generated using ArcGIS Pro proof-of-concept toolbox

The second assessment method involves 3D viewing, a technique described in the previous section in relation to silt fences. A 3D global scene can similarly be a valuable tool for the remote examination of wattles. Panning and zooming close to a wattle, as shown in Figure 30, can indicate how much sediment has accumulated, the cleanliness of the wattle, and possibly the extent to which the wattle has been soaked in sediment over time.



Figure 30. 3D view showing a close-up examination of a wattle

Profile analysis together with 3D viewing is sufficient for monitoring and assessing the current condition of wattle devices.

Stormwater Basins

Stormwater basins are excavated areas designed to collect runoff and release it at a controlled rate, allowing suspended sediment to settle when sufficient detention time is provided. While monitoring the coloration, flooding, and fill level of small basins is achievable through manual foot-on-ground inspection, applying similar inspection techniques to wider basins is challenging. However, adequate data for assessing basins can be obtained from 2D orthophotos, which can indicate flooding conditions and other critical features required for an overall assessment of a basin's conditions. Mediapolis Site 1 featured a few stormwater basins; 2D orthophotos of these devices are provided in Figure 31.



Figure 31. 2D orthophotos showing stormwater basins from Mediapolis Site 1

Additionally, the coverage area of a basin can be extracted from ArcGIS Pro by tracing the perimeter of the basin, as shown in Figure 32. The area feature reflects the basin's expansion and potential water loss over time.

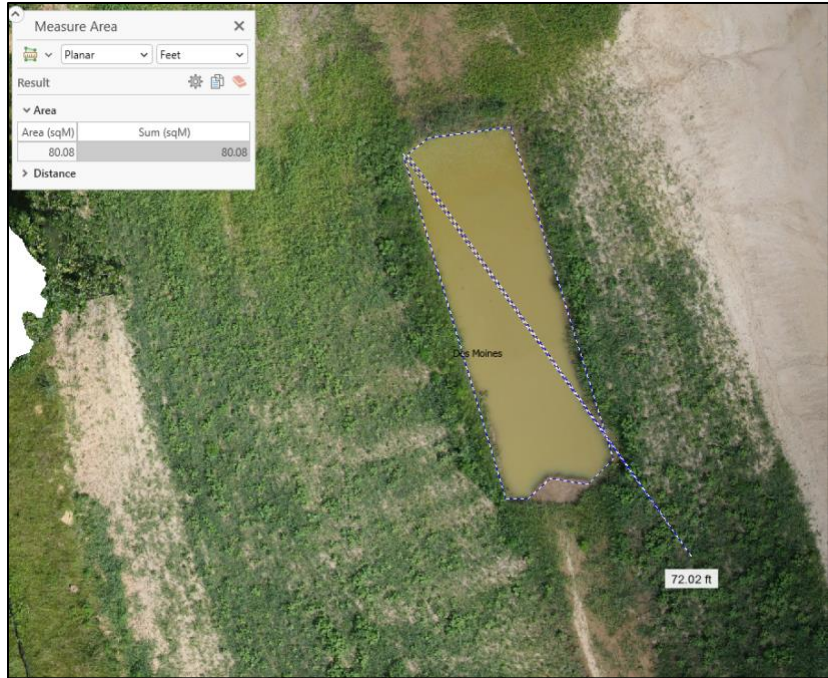


Figure 32. Measurement of the area of a stormwater basin

SUMMARY AND LIMITATIONS

Erosion and sediment control practices are essential for ensuring compliance with U.S. Environmental Protection Agency guidelines and Iowa DOT requirements for construction sites. In this study, we investigated the adoption of sUAS platforms to remotely monitor and assess the condition of ESCDs, with the goal of making the resulting data rapidly available for use by Iowa DOT personnel. We visited two sites in Mediapolis, Iowa, and another site in Oskaloosa, Iowa, to collect data using three different sUAS platforms. The DEM, orthophoto, and multispectral imagery obtained from these site visits provided numerous data sources for assessing ESCD conditions. We learned that traditional field inspections of ESCDs are typically conducted weekly. Therefore, we proposed a prototype workflow and identified key underlying factors for achieving a seamless transition from data collection to data visualization.

We also discovered that sUAS data can serve as digital repository capturing the progression of the entire construction site. Through this database, users such as Iowa DOT construction site monitoring staff can track construction progress and conduct a comprehensive hydrologic analysis to determine the best positions to install ESCDs, detect potential problematic areas, and promptly address issues by installing additional devices before a significant failure occurs.

The major outcomes of this study include the following:

- Developed practical sUAS data collection strategies and a workflow for sUAS data collection and processing to monitor the condition of ESCDs at active construction sites
- Identified critical factors for achieving a rapid and seamless workflow from sUAS data collection to data visualization
- Developed proof-of-concept toolboxes capable of feature extraction for the remote monitoring and assessment of the ESCDs from processed sUAS data
- Proposed suitable analysis methods for the ESCDs identified in this study
- Discussed other potential applications for routine sUAS data collection, including the creation of a rich timestamped digital database capturing the progression of the entire construction site

While this study has demonstrated early successes in remote monitoring and condition assessment, this study's limitations can help shape the direction of future research. These limitations are as follows:

- sUAS technology can be affected by sudden changes in weather conditions during data collection. Although routine weather monitoring before flight operations is recommended, the need to wait for favorable weather conditions limits sUAS deployment to periods of suitable weather
- Compared to the significant number of ESCDs typically installed by the Iowa DOT on construction sites, only five types were present at the sites we visited, limiting the research focus to these devices. Future investigations should include additional ESCD types to

evaluate feature extraction methods suitable for these devices and better understand the potential of sUAS for comprehensive ESCD monitoring.

- Processing sUAS image data from large construction sites requires substantial computational resources to enable timely digital data delivery. Without adequate computing capability, the transition from raw imagery to final analysis may become slow and inefficient.
- The sites visited for data collection featured little to no active construction. More complex scenarios, such as fast-moving construction sites, may create additional challenges for drone teams in setting up an operational base, placing GCPs, and managing non-data-collection workflows, such as image matching and processing during data analysis.
- While this study demonstrates early success in exploring the use of sUAS for ESCD monitoring, further work is required. Future research should include visits to multiple sites with varying terrain and site conditions, testing of the digital delivery workflow, and evaluation of the feature extraction toolboxes across different ESCD types.

FUTURE RESEARCH DIRECTIONS

sUAS data collected from the Mediapolis and Oskaloosa sites were processed and analyzed for condition monitoring and ESCD assessment. Although a seamless transition from data collection to visualization is anticipated if adequate attention is given to the critical factors identified in the Data Collection, Processing, and Visualization chapter, further research is required to comprehensively evaluate the adoption of repetitive high-altitude flights for continuous ESCD assessment.

Similar to traditional field inspections, sUAS platforms should be routinely deployed in future studies for periodic data collection across different sites that feature additional devices beyond those covered in this pilot study.

Different data collection variables should also be explored in future research, including variations in the number of GCPs and the adoption of RTK modules when few or no GCPs are available to deploy or when the use of GCPs is impractical. While GCPs are valuable for maintaining geospatial accuracy, their placement and retrieval during data collection across large construction sites can increase the overall time and effort required to collect sUAS data. Therefore, visiting additional construction sites throughout the year and collecting diverse datasets, including color, thermal, and multispectral imagery, will be critical in determining the optimal number of GCPs required per square foot for effective ESCD monitoring. The Positional Accuracy Standards for Digital Geospatial Data, developed by the American Society for Photogrammetry and Remote Sensing (ASPRS, <https://asprs.org/Main/Main/Standards/Positional-Accuracy-Standards.aspx>), are likely to provide insight into the number of GCPs to deploy for different sUAS data collection efforts. Another factor that could potentially expedite the data collection workflow is to set the image overlap (forward and setting) to a lower level while still meeting accuracy needs for orthophotos and DEMs. Future research should investigate the optimal overlap required to achieve the desired image resolution for adequate ESCD assessment, balancing data quality with processing efficiency.

Another popular complement or alternative to sUAS data collection is the use of satellite imagery for remote sensing. High-resolution multispectral satellite imagery from various public and private platforms should be acquired, potentially along with satellite-derived DEMs, and the workflow from data acquisition to final delivery for ESCD assessment should be compared with that developed in this study for sUAS. The ability of satellite imagery to support the assessment of construction site progress and enable near-real-time evaluation of ESCD conditions should be extensively investigated. The advantages and limitations associated with the use of satellite imagery, along with opportunities for the complementary adoption of both sUAS and satellite technologies, should be systematically assessed in future studies. Such investigations can help establish a practical, rapid, and cost-effective pathway for the broader adoption of remote sensing technologies in ESCD monitoring.

Finally, the automated analyses developed for the five devices covered in this pilot project should be packaged as a software suite, with users logging in for a holistic analysis of the ESCDs

at a given site. In future studies, additional work is needed to develop automated solutions for other devices such as mulch, reinforcement mats, and other ESCDs not found at the three sites visited for this pilot study.

Beyond ESCD monitoring, construction activities would also benefit from periodic aerial data collection for tasks such as earth volume monitoring and the tracking of completed work. Therefore, it is proposed that overall construction activity monitoring be incorporated into future research studies for further investigation and the development of practical guidelines.

In summary, subsequent future research should focus on the following:

- Development of a practical workflow for the large-scale detection and quantification of ESCD features using shorter flight times for sUAS data collection efforts
- Evaluation of the use of satellite imagery for ESCD monitoring
- Development of a software suite with different automatic feature extraction logics for the quantitative assessment of ESCDs

REFERENCES

- Banić, M., A. Miltenović, M. Pavlović, and I. Ćirić. 2019. Intelligent machine vision based railway infrastructure inspection and monitoring using UAV. *Facta Universitatis, Series: Mechanical Engineering*, Vol. 17, No. 3, pp. 357–364. <https://doi.org/10.22190/FUME190507041B>.
- Bannari, A., D. Morin, F. Bonn, and A. R. Huete. 1995. A review of vegetation indices. *Remote Sensing Reviews*, Vol. 13, Nos. 1–2, pp. 95–120. <https://doi.org/10.1080/02757259509532298>.
- Brooks, C., C. Cook, R. Dobson, T. Oommen, K. Zhang, A. Mukherjee, R. Samsami, A. Semenchuk, B. Lovelace, and V. Hung. 2022. *Integration of Unmanned Aerial Systems Data Collection into Day-to-Day Usage for Transportation Infrastructure—A Phase III Project*. Michigan Tech Transportation Institute. <https://rosap.ntl.bts.gov/view/dot/62974>.
- Bugg, R. A., W. Donald, W. Zech, and M. Perez. 2017. Performance evaluations of three silt fence practices using a full-scale testing apparatus. *Water*, Vol. 9, No. 7, pp. 502. <https://doi.org/10.3390/w9070502>.
- Carabassa, V., P. Montero, J. M. Alcañiz, and J.-C. Padró. 2021. Soil erosion monitoring in quarry restoration using drones. *Minerals*, Vol. 11, No. 9, p. 949. <https://doi.org/10.3390/min11090949>.
- Castillo, V. M., W. M. Mosch, C. C. García, G. G. Barberá, J. A. N. Cano, and F. López-Bermúdez. 2007. Effectiveness and geomorphological impacts of check dams for soil erosion control in a semiarid Mediterranean catchment: El Cárcavo (Murcia, Spain). *CATENA*, Vol. 70, No. 3, pp. 416–427. <https://doi.org/10.1016/j.catena.2006.11.009>.
- Cooke, S. J., J. M. Chapman, and J. C. Vermaire. 2015. On the apparent failure of silt fences to protect freshwater ecosystems from sedimentation: A call for improvements in science, technology, training and compliance monitoring. *Journal of Environmental Management*, Vol. 164, pp. 67–73. <https://doi.org/10.1016/j.jenvman.2015.08.033>.
- Fischer, S., E. Lawless, J. Lu, and K. Van Fossen. 2020. *Global Benchmarking Study on Unmanned Aerial Systems for Surface Transportation: Domestic Desk Review*. Federal Highway Administration. <https://www.fhwa.dot.gov/uas/hif20091.pdf>.
- Flammini, F., C. Pragliola, and G. Smarra. 2016. Railway infrastructure monitoring by drones. International Conference on Electrical Systems for Aircraft, Railway, Ship Propulsion and Road Vehicles and International Transportation Electrification Conference (ESARS-ITEC), November 2–4, Toulouse, France.
- Huang, S., L. Tang, J. P. Hupy, Y. Wang, and G. Shao. 2021. A commentary review on the use of normalized difference vegetation index (NDVI) in the era of popular remote sensing. *Journal of Forestry Research*, Vol. 32, No. 1, pp. 1–6. <https://doi.org/10.1007/s11676-020-01155-1>.
- Kastridis, A., S. Margiorou, and M. Sapountzis. 2022. Check-dams and silt fences: Cost-effective methods to monitor soil erosion under various disturbances in forest ecosystems. *Land*, Vol. 11, No. 12, 2129. <https://doi.org/10.3390/land11122129>.
- Kazaz, B., S. Poddar, S. Arabi, M. A. Perez, A. Sharma, and J. B. Whitman. 2021. Deep learning-based object detection for unmanned aerial systems (UASs)-based inspections of construction stormwater practices. *Sensors*, Vol. 21, No. 8, 2834. <https://doi.org/10.3390/s21082834>.

- Liu, L., M. A. Perez, J. B. Whitman, W. N. Donald, and W. C. Zech. 2021. SILTspread: Performance-based approach for the design and installation of silt fence sediment barriers. *Journal of Irrigation and Drainage Engineering*, Vol. 147, No. 10, 04021041. [https://doi.org/10.1061/\(ASCE\)IR.1943-4774.0001608](https://doi.org/10.1061/(ASCE)IR.1943-4774.0001608).
- Mahmud, A. R. 2021. Soil erosion and sedimentation control using biological methods. *International E-Conference on Applied Sciences, Society and Economics 2021 (ICASSE2021)*, pp. 153–159. Conference Asia Network.
- Margiorou, S., A. Kastridis, and M. Sapountzis. 2022. Pre/post-fire soil erosion and evaluation of check-dams effectiveness in Mediterranean suburban catchments based on field measurements and modeling.” *Land*, Vol. 11, No. 10, 1705. <https://doi.org/10.3390/land11101705>.
- Masi, E. B., S. Segoni, and V. Tofani. 2021. Root reinforcement in slope stability models: A review. *Geosciences*, Vol. 11, No. 5, 212. <https://doi.org/10.3390/geosciences11050212>.
- Mitra, R., M. A. A. Sourav, S. Kim, B. Gulmezoglu, and H. Ceylan. 2025. Comparative case study: Traffic monitoring using YOLOv11-based object detection and two tracking algorithms with small uncrewed aerial systems. International Conference on Transportation and Development 2025, pp. 311–321. American Society of Civil Engineers. <https://doi.org/10.1061/9780784486191.027>.
- Nooralishahi, P., C. Ibarra-Castanedo, S. Deane, F. López, S. Pant, M. Genest, N. P. Avdelidis, and X. P. V. Maldague. 2021. Drone-based non-destructive inspection of industrial sites: A review and case studies. *Drones*, Vol. 5, No. 4, pp. 106. <https://doi.org/10.3390/drones5040106>.
- Oguntoye, K. S., S. Laflamme, R. Sturgill, and D. J. Eisenmann. 2023. Review of artificial intelligence applications for virtual sensing of underground utilities. *Sensors*, Vol. 23, No. 9, 4367. <https://doi.org/10.3390/s23094367>.
- Oguntoye, K. S., M. A. A. Sourav, R. Mitra, A. Jenkins, H. Ceylan, S. Kim, B. Gulmezoglu, Y. Mo, and C. Brooks. 2025. Low-altitude sUAS flights for remote sensing of submillimeter hairline cracks: A case study. International Conference on Transportation and Development 2025, pp. 800–809. American Society of Civil Engineers. <https://doi.org/10.1061/9780784486191.070>.
- Olivetti, D., H. Roig, J.-M. Martinez, H. Borges, A. Ferreira, R. Casari, L. Salles, and E. Malta. 2020. Low-cost unmanned aerial multispectral imagery for siltation monitoring in reservoirs. *Remote Sensing*, Vol. 12, No. 11, 1855. <https://doi.org/10.3390/rs12111855>.
- Osterkamp, W. R., C. R. Hupp, and M. Stoffel. 2012. The interactions between vegetation and erosion: new directions for research at the interface of ecology and geomorphology. *Earth Surface Processes and Landforms*, Vol. 37, No. 1, pp. 23–36. <https://doi.org/10.1002/esp.2173>.
- Pietersen, R. A., M. S. Beauregard, and H. H. Einstein. 2022. Automated method for airfield pavement condition index evaluations. *Automation in Construction*, Vol. 141. <https://doi.org/10.1016/J.AUTCON.2022.104408>.
- Puigdefábregas, J. 2005. The role of vegetation patterns in structuring runoff and sediment fluxes in drylands. *Earth Surface Processes and Landforms*, Vol. 30, No. 2, pp. 133–147. <https://doi.org/10.1002/esp.1181>.
- Risse, L. M., S. A. Thompson, J. Governo, and K. Harris. 2008. Testing of new silt fence materials: A case study of a belted strand retention fence. *Journal of Soil and Water Conservation*, Vol. 63, No. 5, pp. 265–273. <https://doi.org/10.2489/jswc.63.5.265>.

- Sourav, M. A. A., H. Ceylan, C. Brooks, R. Dobson, S. Kim, D. Peshkin, and M. Brynick. 2024. Use of small unmanned aircraft systems in airfield pavement inspection: Implementation and potential. *International Journal of Pavement Engineering*, Vol. 25, No. 1. <https://doi.org/10.1080/10298436.2024.2401630>.
- Sourav, M. A. A., H. Ceylan, C. Brooks, D. Peshkin, S. Kim, R. Dobson, C. Cook, M. Mahedi, and A. Jenkins. 2023a. *Small Unmanned Aircraft System for Pavement Inspection*. DOT/FAA/TC-23/50. Federal Aviation Administration.
- Sourav, M. A. A., H. Ceylan, S. Kim, C. Brooks, D. Peshkin, R. Dobson, and M. Brynick. 2023b. Use of digital elevation model for detecting airfield pavement distress. *Airfield and Highway Pavements 2023*, pp. 254–265. American Society of Civil Engineers. <https://doi.org/10.1061/9780784484906.024>.
- Sourav, M. A. A., H. Ceylan, S. Kim, C. Brooks, D. Peshkin, R. Dobson, M. Brynick, and M. DiPilato. 2022. Small uncrewed aircraft systems-based orthophoto and digital elevation model creation and accuracy evaluation for airfield portland cement concrete pavement distress detection and rating. *International Conference on Transportation and Development 2022*, pp. 168–180. American Society of Civil Engineers. <https://doi.org/10.1061/9780784484371.016>.
- Sourav, M. A. A., M. Mahedi, H. Ceylan, S. Kim, C. Brooks, D. Peshkin, R. Dobson, and M. Brynick. 2023c. Evaluation of small uncrewed aircraft systems data in airfield pavement crack detection and rating. *Transportation Research Record*, Vol. 2677, No. 1, pp. 653–668. <https://doi.org/10.1177/03611981221101030>.
- Tan, Y., and Y. Li. 2019. UAV photogrammetry-based 3D road distress detection. *ISPRS International Journal of Geo-Information*, Vol. 8, No. 9, p. 409. <https://doi.org/10.3390/ijgi8090409>.
- Theofanidis, A., A. Kastridis, and M. Sapountzis. 2025. Effectiveness of torrential erosion control structures (check dams) under post-fire conditions—The importance of immediate construction. *Land*, Vol. 14, No. 3, 629. <https://doi.org/10.3390/land14030629>.
- Vidyadharan, A., T. Carter, H. Ceylan, C. Bloebaum, K. Gopalakrishnan, and S. Kim. 2017. Civil infrastructure health monitoring and management using unmanned aerial systems. *Airfield and Highway Pavements 2017*, pp. 207–216. American Society of Civil Engineers. <https://doi.org/10.1061/9780784480946.019>.
- Watts, A. C., V. G. Ambrosia, and E. A. Hinkley. 2012. Unmanned aircraft systems in remote sensing and scientific research: Classification and considerations of use. *Remote Sensing*, Vol. 4, No. 6, pp. 1671–1692. <https://doi.org/10.3390/rs4061671>.
- Whitman, J. B., J. C. Schussler, M. A. Perez, and L. Liu. 2021. Hydraulic performance evaluation of wattles used for erosion and sediment control. *Journal of Irrigation and Drainage Engineering*, Vol. 147, No. 7, 04021028. [https://doi.org/10.1061/\(ASCE\)IR.1943-4774.0001586](https://doi.org/10.1061/(ASCE)IR.1943-4774.0001586).
- Xue, J., and B. Su. 2017. “Significant remote sensing vegetation indices: A review of developments and applications.” *Journal of Sensors*, Vol. 2017, No. 1, 1353691. <https://doi.org/10.1155/2017/1353691>.
- Yeri, S., B. Barfield, E. Stevens, K. Gasem, J. Arjunan, M. Matlock, and J. Hayes. 2012. FAEST, a new silt fence technology for construction sites. *Impacts of Global Climate Change*, pp. 1–12. American Society of Civil Engineers. [https://doi.org/10.1061/40792\(173\)184](https://doi.org/10.1061/40792(173)184).

- Young, S. S., S. Rao, and K. Dorey. 2021. Monitoring the erosion and accretion of a human-built living shoreline with drone technology. *Environmental Challenges*, Vol. 5, 100383. <https://doi.org/10.1016/j.envc.2021.100383>.
- Zhang, X., Y. Fu, Q. Pei, J. Guo, and S. Jian. 2024. Study on the root characteristics and effects on soil reinforcement of slope-protection vegetation in the Chinese Loess Plateau. *Forests*, Vol. 15, No. 3, 464. <https://doi.org/10.3390/f15030464>.
- Zuazo, V. H. D., and C. R. R. Pleguezuelo. 2009. Soil-erosion and runoff prevention by plant covers: A review. *Sustainable Agriculture*, pp. 785–811. Eds. E. Lichtfouse, M. Navarrete, P. Debaeke, S. Véronique, and C. Alberola. Springer Netherlands.

**THE INSTITUTE FOR TRANSPORTATION IS THE FOCAL POINT FOR TRANSPORTATION
AT IOWA STATE UNIVERSITY.**

InTrans centers and programs perform transportation research and provide technology transfer services for government agencies and private companies;

InTrans contributes to Iowa State University and the College of Engineering's educational programs for transportation students and provides K–12 outreach; and

InTrans conducts local, regional, and national transportation services and continuing education programs.



**IOWA STATE
UNIVERSITY**

Visit InTrans.iastate.edu for color pdfs of this and other research reports.